Adaptive and Autonomous Protocol for Spectrum Identification and Coordination in Ad hoc Cognitive Radio Network

BY

Henry Ohiani Ohize

A thesis submitted for the degree of

Doctor of Philosophy

in the Department of Electrical Engineering,

Faculty of Engineering and the Built Environment, University of Cape Town

December 2017

Supervisor: Associate Professor Mqhele DLODLO

Dedication

To my lovely wife Comfort and daughters Oiza and Onize.

To my supportive parents, Professor and Mrs Ohize.

To my inspirational siblings, Mrs Helen Abu, Dr Stephen and Dr Victor.

Acknowledgements

First and foremost, my appreciation goes to God Almighty for the gift of life.

I am greatly indebted to my supervisor Professor Mqhele Dlodlo. Your style of supervision and mentorship gave me the confidence in exploring my imaginations. Many thanks for your comments, corrections and suggestions throughout the course of this study.

My sincere appreciation is extended to my colleagues who have shared their valuable suggestions and evaluations throughout the course of this work; Dr A. J. Onumanyi, Dr Sesham Srinu, Engr Habeeb Belo-Salau, Mr Enoruwa Obayiuwana, Engr Opeyemi Osanaiye. Engr Babatunde Ogunleye, Engr Mary Adedoyin, Engr. Bima Muhammed, Engr Michael Okwori and Mr Lerato Mohapi.

I am immensely thankful to my employer, the Federal University of Technology (FUT) Minna, Nigeria for granting me this great opportunity and for supporting me throughout my study. Special thanks to the following staff of FUT Minna, Professor M. Akanji, Vice-Chancellor; Professor S. Sadiku, the Dean, School of Engineering and Engineering Technology; Professor B. Adegboye, Head of Department, Electrical and Electronics Engineering; Professor E.N. Onwuka, Head of Department, Telecommunication Engineering; A/Professor M.N Nwohu, Engr A. Raji, Dr Abraham, Engr J. Ambafi, Engr, D. Umar, Engr. L. Olatomiwa, Engr A.

Achonu, Dr C. Alenoghena, Dr M. Zungeru, Engr B. Ajagun, Engr. A. Ashraf and the entire staff of Electrical and Electronics Engineering, FUT, Minna.

My gratitude to members of the COMMED Research Group and CRG Group in the Department of Electrical Engineering at the University of Cape Town. I am particularly grateful to Mr Nyasha Mukudu, Mr Ayo Periola, Mr Neco Ventura, Dr Olabisi Falowo, Mrs Joyce Mwangama, Mr Joseph Orimolade, Mrs Elizabeth Okumu, Mrs Didaciane Mukanyikigira, Mr Angus Brandt, Mr Uyoata Uyoata, Mrs Ojuetimi Akinsolu, Mr Adeyemi Oluwadamilare, Mr Chales Lubobya, Mr Joshua Adeleke, Mr Fredrick Kumi, Mr John Rowdzi, Mr Nixon Ng'ethe, Mr Elisha Amakan, Mr Micheal Terefa.

My gratitude also extends to the following members of staff of the Electrical Department at the University of Cape Town; Prof. Edward Boje, Head of Department, Mrs. Nicole Moodley, Mrs Rachmat Harris, Mrs Carol Koonin, Mrs Janine Buxey and Mr Pierre Bizimana Thanks for your support.

I would like to acknowledge all the anonymous reviewers and the team of external assessors in the course of the work. You have indeed contributed immensely to the value and final output of this thesis.

My gratitude would be incomplete without mentioning friends that have contributed greatly to making this journey an easier one for me; Special thanks to Pastor and Mrs Oluremi Adelusi, Engr Tade Durojaye, Deacon and Mrs Shenu Ogundipe, Dr and Mrs Adeniyi Isafiade, Dr Lukman Oyewobi, Mr Ganiyu Bashiru, Mr Mohammed Alhassan, Engr Abdulkadir Ibrahim, Dr and Mrs Ikenna Ireka, Mrs Chidima Ojemma and Family, Miss Bukola Awodele, Mr Abubakar Abdulkadir, Engr Olurotimi Awodeji and Bar Antony Diala.

Finally, a very special thank you to my family for your unwavering support; my lovely wife, Comfort Ohize; my dear parents, Professor and Mrs E. Ohize; my beloved Sister Mrs H. Abu and My fantastic brothers Dr Victor and Dr Stephen.

Abstract

The decentralised structure of wireless Ad hoc networks makes them most appropriate for quick and easy deployment in military and emergency situations. Consequently, in this thesis, special interest is given to this form of network. Cognitive Radio (CR) is defined as a radio, capable of identifying its spectral environment and able to optimally adjust its transmission parameters to achieve interference free communication channel. In a CR system, Dynamic Spectrum Access (DSA) is made feasible. CR has been proposed as a candidate solution to the challenge of spectrum scarcity. CR works to solve this challenge by providing DSA to unlicensed (secondary) users. The introduction of this new and efficient spectrum management technique, the DSA, has however, opened up some challenges in this wireless Ad hoc Network of interest; the Cognitive Radio Ad Hoc Network (CRAHN). These challenges, which form the specific focus of this thesis are as follows: First, the poor performance of the existing spectrum sensing techniques in low Signal to Noise Ratio (SNR) conditions. Secondly the lack of a central coordination entity for spectrum allocation and information exchange in the CRAHN. Lastly, the existing Medium Access Control (MAC) Protocol such as the 802.11 was designed for both homogeneous spectrum usage and static spectrum allocation technique.

Consequently, this thesis addresses these challenges by first developing an algorithm comprising of the Wavelet-based Scale Space Filtering (WSSF) algorithm and the Otsu's multi-threshold algorithm to form an Adaptive and Autonomous Wavelet-Based Scale Space Filter (AWSSF) for Primary User (PU) sensing in CR. These combined algorithms produced an enhanced algorithm that improves detection in low SNR conditions when compared to the performance of EDs and other spectrum sensing techniques in the literature. Therefore, the AWSSF met the performance

requirement of the IEEE 802.22 standard as compared to other approaches and thus considered viable for application in CR.

Next, a new approach for the selection of control channel in CRAHN environment using the Ant Colony System (ACS) was proposed. The algorithm reduces the complex objective of selecting control channel from an overtly large spectrum space,to a path finding problem in a graph. We use pheromone trails, proportional to channel reward, which are computed based on received signal strength and channel availability, to guide the construction of selection scheme. Simulation results revealed ACS as a feasible solution for optimal dynamic control channel selection.

Finally, a new channel hopping algorithm for the selection of a control channel in CRAHN was presented. This adopted the use of the bio-mimicry concept to develop a swarm intelligence based mechanism. This mechanism guides nodes to select a common control channel within a bounded time for the purpose of establishing communication. Closed form expressions for the upper bound of the time to rendezvous (TTR) and Expected TTR (ETTR) on a common control channel were derived for various network scenarios. The algorithm further provides improved performance in comparison to the Jump-Stay and Enhanced Jump-Stay Rendezvous Algorithms. We also provided simulation results to validate our claim of improved TTR.

Based on the results obtained, it was concluded that the proposed system contributes positively to the ongoing research in CRAHN.

Contents

List of Tables

List of Figures

List of Abbreviations

ACO	Ant Colony Optimization
ACS	Ant Colony System
A/D	Analogue to Digital
AHN	Ad hoc Network
AR	Auto Regression
AS	Ant System
ATT	Adaptive Threshold Technique
AWGN	Additive white Gaussian noise
AWSSF	Adaptive Wavelet Scale Space Filter
BER	Bit Error Rate
CC	Control Channel
CCC	Common Control Channel
CFD	Cyclostationary Feature Detection
CH	Channel Hopping
CHS	Channel Hopping Sequence
CR	Cognitive Radio
CRAHN	Cognitive Radio Ad hoc Network
DCCC	Dynamic Common Control Channel
DFT	Discrete Fourier Transform
DTV	Digital Television
DWPT	Discrete Wavelet Packet Transform
DSA	Dynamic Spectrum Access
DSAP	Dynamic Spectrum Access Protocol
EA	Evolution Algorithm
ED	Energy Detector
ETTA	Expected Time To Rendezvous
EJS	Enhance Jump-Stay
FDM	Frequency Division Multiplexing
FCC	Federal Communication Commission
FFT	Fast Fourier Transform
GA	Genetic Algorithm
GMM	Gaussian Mixture Model

HIA	Hole Information Array
ISM	Industrial Scientific and Medical
JS	Jump-Stay
KNN	K-nearest neighbour
LTI	Linear Time-Invariant
LU	Licensed User
MA	Memetic Algorithm
MAC	Medium Access Protocol
MCA	Modular Clock Algorithm
MF	Match Filter
ML	Machine Learning
MMCA	Modified MCA
MME	Maximum-Minimum Eigenvalue
MTM-SVD	Multitaper-Singular Value Decomposition
NP	Neyman-Pearson
OFDM	Orthogonal Frequency Division Multiplexing
OFDMA	Orthogonal Frequency Multiple Access
PCA	Principal Component Analysis
PSD	Power Spectral Density
PSO	Particle Swarm Optimisation
PU	Primary User
QoS	Quality of Service
RAM	Random Access Memory
ROC	Receiver Output Curve
ROHT	Recursive One-Sided Hypothesis Test
RSS	Received Signal Strength
SA	Spectrum Access
SASJ	Swarm Aided Stay-Jump
SFLA	Shuffled Frog Leaping Algorithm
SHIA	Spectrum Hole Information Array
SI	Spectrum Identification
SNR	Signal to Noise Ratio
SS	Spectrum Sensing
SU	Secondary User
SVM	Support Vector Machine
TCT	Time-Cost Trade-off
TTA	Time To Rendezvous
UWB	Ultra Wide band
VNI	Visual Networking Index
WSSF	Wavelet Scale Space Filter
WT	Wavelet Transform

Chapter 1

General Introduction

Radio spectrum used for wireless communication has begun to experience congestion as shown by recent observations. Spectrum scarcity is imminent, and this has raised concerns in the research communities. Cisco VNI, a software development and research agency has described a further explosion of Wireless traffic in the nearest future. This sudden problem of spectrum scarcity is a result of the recent gush in wireless communication technology deployment. Furthermore, the introduction of more bandwidth demanding multimedia services [1] has added to this spectrum scarcity. Noteworthy is that the current command and control technique used globally for spectrum allocation to subscribers has some inherent drawbacks and as such proven rather inefficient in the face of this looming spectrum scarcity [2]. Some of the intrinsic drawbacks include, but not limited to, are first, its inability to recover bands which have been allocated to radio technologies that are outdated. Secondly, this technique has failed to identify underutilised bands, therefore, resulting in spectrum scarcity. The solution to this is the development of an alternative and efficient spectrum management technique [3].

Consequently, two major solutions that address this challenge of spectrum scarcity are; Migration from Analogue to Digital Television (DTV) transmission to free-up large usable TV spectrum [4, 5, 6] and Cognitive Radio Technology [7, 8, 9, 10]. Migration from Analogue to DTV, though feasible, this solution has its intrinsic drawback. This drawback is associated with the use of the same traditional spectrum allocation technique which is presumably responsible for the current pseudo spectrum scarcity condition. Thus there exists the possibility of re-exhausting retracted frequencies [3]. Cognitive Radio is the second and most prominent solution drawing most attention among researchers and industry players as a more lasting and sustainable solution to the challenge of spectrum scarcity [11, 12, 13, 14].

CR technology provides a paradigm shift from the tradition fixed spectrum allocation technique. CR allows for Dynamic Spectrum Access (DSA) [15, 16]. DSA implies that unlicensed (secondary) users (SU) are allowed an opportunistic use of the licensed white space spectrum [17]. DSA will eventually increase spectrum usage efficiency and reduce congestion. However, promoters of the CR technology are confronted with the challenges involved in the development of a fully functional CR system. The CR is associated with the complex requirements for the integration of the major building blocks of CR namely Spectrum Identification (Sensing), Spectrum Access, Spectrum Sharing and Spectrum Management [18, 3].

Therefore, in this research, the focus is geared towards key enhancements and contributions to the Spectrum Identification (SI) and Spectrum Access (SA) blocks of the Cognitive Radio Ad hoc Network (CRAHN) of interest.

In this research, first of all, special emphasis is laid on spectrum identification, because it forms the basis for CR operation. After that, focus is laid on coordinating the secondary user's (SU's) to avoid co-tier (among other SUs) and cross-tier (with PU) interference.

In CR, Spectrum Identification refers to the detection of PU signals in the presence of noise. The SI task is formulated as a discriminate analysis of the following two binary hypotheses H_0 and H_1

$$H_0 : y(t) = n(t) \quad \text{Absence of Primary user,} \tag{1.1}$$

$$H_1 : y(t) = s(t) + n(t) \quad \text{Presense of Primary, user} \tag{1.2}$$

where $y(t)$ represent the measured test statics, $s(t)$ is the PU modulated signal and $n(t)$ is an Additive White Gaussian Noise (AWGN). Therefore the key objective here is to develop a robust, adaptive and autonomous spectrum sensing algorithm that will complement the Energy Detector (ED) technique in low Signal to Noise Ratio (SNR) scenario.

Lastly, the spectrum access module of CRAHN is addressed. The core functions of spectrum access in CRAHN are interference control and collision avoidance to PUs and amongst SUs respectively. These functions are implemented as a protocol in the Medium Access Control (MAC) layer [19, 20]. However, despite the peculiarity of CRAHN, such as spectrum heterogeneity, spatial and time varying nature of spectrum, the research and industrial community still face a Herculean task in the full implementation and deployment of CRAHN. Several MAC protocol designs have been proposed for centralised network architectures such as the 802.22 and Dynamic Spectrum Access Protocol (DSAP)[21, 22, 23]. However, few have been designed for distributed networks also known as Ad-Hoc Networks. This stems from implementation issues ranging from coordination issues to QoS issues.

The coordination issues include SU to SU and PU to SU interference management, multichannel hidden node, broadcast and multicast issues, spectrum information distribution, channel access, receiver and transmitter synchronisation etc. The

introduction of a fixed or preselected control channel, in MAC protocol design is the most popular proposed solution. However, this proposed solution has opened up even more challenging issues such as control channel security, robustness to PU activities, control channel coverage and control channel saturation [24]. In our work, the use of a flexible or dynamic control channel was proposed. This flexible control channel will thoroughly address issues mentioned above. The key contribution here is the introduction of a control channel selection algorithm based on Swarm Intelligence with bounded time to rendezvous (TTR).

1.1 Motivation for the Research

Self-organising networks such as CRHAN will find great and tremendous applications in situations where no infrastructure is available e.g. in disaster areas where existing infrastructure has been damaged or where the cost of setting up infrastructure is too high and probably temporary.

Other possible areas of application of this work include, collaborative and distributed computing e.g. quick communication with minimal configuration among a group of people. Also, emergency operations such as rescue, crowd control, and military operations.

1.2 Statement of the Problem

In this thesis, the following specific problems were addressed:

1. For CR operation, the is a need for fast and accurate spectrum detection. The popular ED technique in literature performs poorly in low Signal to Noise Ratio

(SNR) conditions. The ED's poor performance at low SNR is attributed to the proximity of threshold value to noise floor in a bid to detect signal, thereby leading to the misclassification of PU signals, consequently a high rise in the rate of false alarm. Hence there is a need to complement the ED's performance with a spectrum sensing technique that would perform better at low SNR. In an attempt to improve detection in low SNR conditions, we considered the use of Wavelet-based Scale Space Filtering (WSSF) algorithm to solve this problem.

2. To deploy a fully functional CR, the CR technology must be both adaptive and autonomous in the classification of the spectrum. Consequently, the use of Otsu's multi-threshold algorithm within the WSSF was proposed to achieve dynamism. This novel construction led to an Adaptive Wavelet-based Scale Space Filtering (AWSSF) algorithm presented in Chapter 3.

3. While most works on CR have focused on infrastructure based networks, little has been done on the Ad-hoc based option. This might be attributed to certain existing problems that are closely related to the heterogeneous nature of the spectrum environment (including spatial and time variations), co-tier and cross-tier interference and the overtly large spectrum space to be searched for channel convergence in an Ad hoc set-up. Consequently, our research is motivated by the need to improve on the time to converge on a common coordination channel for CR nodes involved in an Ad-hoc network. Therefore, this work developed a dynamic control channel selection scheme based on swarm intelligence.

1.3 Research Aim and Objectives

The aim of this research is first to develop an adaptive and an autonomous spectrum sensing technique that will complement the ED in low SNR conditions. Secondly to

develop a MAC protocol with flexible control channel that will guarantee efficient spectrum access and coordination for Cognitive radios in a self-deployed Network without interference to both licensed users and other cognitive users.

To achieve the set aim, the following objectives have been highlighted

1. To develop a wavelet-based scale space filtering (WSSF) technique for spectrum sensing
2. To incorporate Otsu's multi-threshold algorithm for use within the WSSF algorithm to introduce dynamism.
3. To develop a control channel selection algorithm using swarms intelligence.
4. To develop an analytical model of the control channel and use the Time to Rendezvous (TTR) metric to evaluate the performance of the model.

1.4 Scope of the Research

The scope of this research is limited to CRAHN. We consider the spectrum access mode as an overlay MAC protocol, where SUs dynamically access the licensed spectrum when PUs do not use it. Zhang Y. *et al.* classified the overlay mode MAC protocols into two subcategories: Centralised MAC and Distributed or Ad Hoc MAC [25, 26]. Of interest, is the distributed MAC protocol. Distributed MAC protocols, unlike the centralised MAC protocols, work without a central coordinator (access point or base station), thus the need for an agreed common control channel for coordination purposes. Our designed MAC protocol falls into this category.

1.5 Research Contributions

This thesis provides the following contributions to knowledge:

1. Application of Wavelet transform for filter design in Cognitive Radio Network, spectrum sensing.

2. Application of an Adaptive and Autonomous threshold estimation technique based on Otsu's multi-threshold technique. The Otsu's threshold technique is popular in image processing.

3. Modelling the control channel selection problem in CRAHN as a path finding problem in a graph.

4. We adopt the use of the bio-mimicry concept to develop a swarm intelligence based mechanism, which will guide nodes seeking to initiate communication, in selecting a common control channel within a bounded time.

1.6 List of Publication

Some of the contributions listed in section 1.5 have been submitted or accepted for publication. The complete list of articles associated with this thesis is presented below.

1. Henry Ohize and Mqhele Dlodlo., *AntMAC:A Dynamic Control Channel Selection MAC Protocol Design for Cognitive Radio Ad Hoc Network.* In the proceedings of South Africa Telecommunication Networks and Application Conference (SATNAC). Nelson Mandela Bay, South Africa 2014.

2. Henry Ohize and Mqhele Dlodlo.,*Ant Colony System Based Control Channel Selection Scheme for Guaranteed Rendezvous in Cognitive Radio Ad-hoc Network*. In the proceedings of the 27th Annual IEEE International Symposium on Personal, Indoor and Mobile Radio Communications (PIMRC), Valencia, Spain 2016.

3. Henry Ohize and Mqhele Dlodlo. *Dynamic Control Channel MAC for Cognitive Radio Ad-Hoc Network: Ant Colony System Implementation*. In the proceedings of the annual Southern Africa Telecommunication Networks and Applications Conference (SATNAC), Fancourt,George, Western Cape, South Africa 2016.

4. Henry Ohize, Mqhele Dlodlo, Adeiza Onumanyi and Habeeb Salau.,*An Adaptive Wavelet-based Scale Space Filtering Algorithm for Spectrum Sensing in Cognitive Radio*. In the proceedings of IEEE Wireless Communications and Networking Conference (WCNC), San Francisco, CA, USA 2017.

5. Henry Ohize and Mqhele Dlodlo.,*A Channel Hopping Algorithm for Guaranteed Rendezvous in Cognitive Radio Ad hoc Networks Using Swarm Intelligence* accepted in Wireless Personal Communications Journal, Springer, 2017.

1.7 Thesis outline

The rest of the thesis is organised as follows: Chapter 2 discusses the relevant literature sources; this is followed by the proposed autonomous and adaptive spectrum sensing technique in Chapter 3. Chapter 4 describes the adaptation of Ant Colony System in CRAHN and Chapter 5 presents the novel channel hopping algorithm while the conclusions are drawn in Chapter 6.

Chapter 2

Background and Overview

2.1 Introduction

This chapter presents a background and an overview of the techniques and technologies, related to the development of this thesis.

2.2 Cognitive Radio Technology

Cognitive radio technology is widely seen as the most feasible solution to the spectrum management problem in wireless communication [27, 28, 29, 30, 31]. The term cognitive radio (CR) was first defined by Mitola in 1999, as a novel technology, which improves spectrum utilisation by seeking and opportunistically utilising radio resources in time, frequency and space domains on a real time base [32].

CR is capable of providing Dynamic Spectrum Access (DSA), a paradigm shift from the traditional fixed spectrum allocation technique. Figure 2.1 gives an illustration

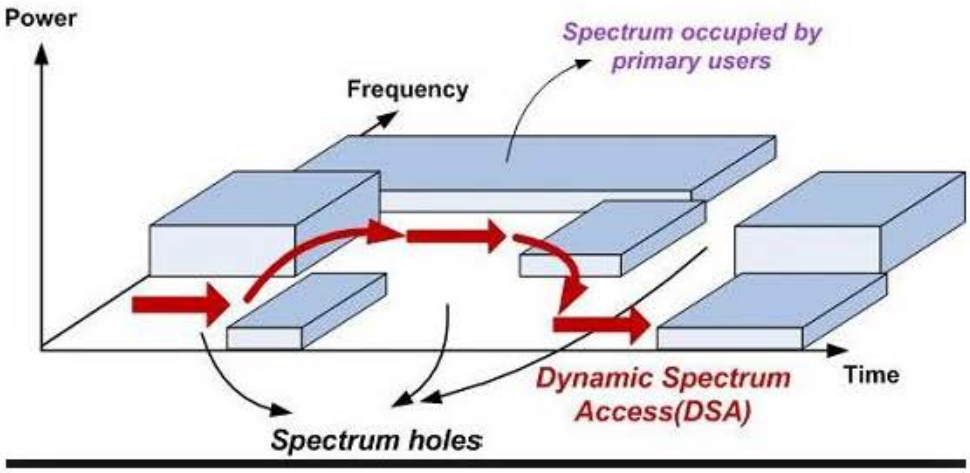

Figure 2.1: Dynamic Spectrum Access enabled by CR.[33]

of DSA enabled by CR. In realising DSA, four key building blocks of CR technology must be addressed and integrated, they include [21];

1. Spectrum Sensing/Identification.
2. Spectrum Access/Coordination.
3. Spectrum Sharing.
4. Spectrum Management and Policy.

In this research work, the emphasis is laid on Spectrum Sensing/Identification and Spectrum Access/Coordination modules of CR as it applies to CRAHN.

2.3 Cognitive Radio Ad Hoc Network (CRAHN)

Ad-hoc networks are decentralised networks, characterised by an absence of a central coordinating node or entity such as an access point or a base station. These networks are self-organizing and can be deployed without infrastructure support see Fig. 2.2a. Ad-hoc networks support various standards. However, the current state of

implementation is limited to the industrial, scientific and medical bands ISM (900 MHz and 2.5 GHz). These bands are becoming congested as a result of an increasing surge in wireless communication technology deployment and the proliferation of newer bandwidth consuming multimedia services. Consequently, the concept of CR has been proposed as a candidate solution. CR allows the opportunistic use of licensed band, by secondary users (opportunistic/unlicensed users) thereby providing DSA for Ad-hoc networks.

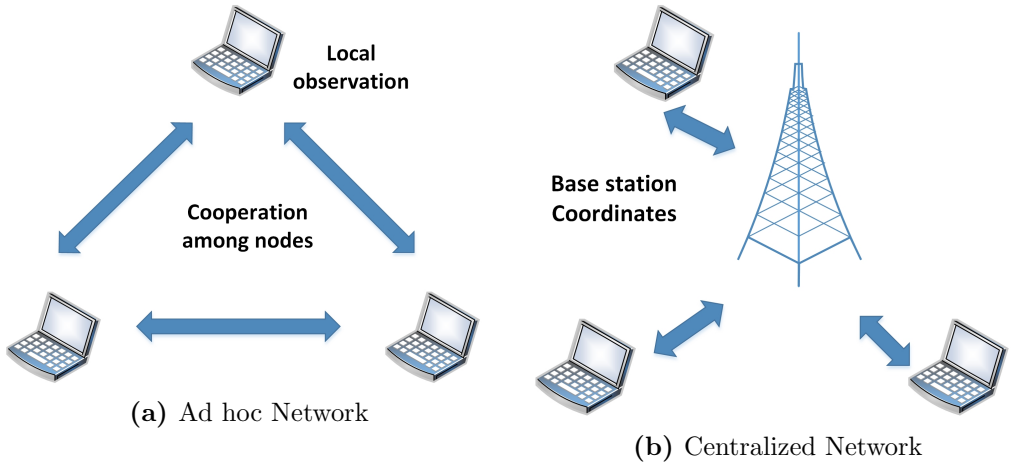

(a) Ad hoc Network

(b) Centralized Network

Figure 2.2: Comparison Between An Adhoc Network and Centralized Network

Unlike the traditional ad-hoc networks (AHN), CRAHNs are characterised by distributed multi-hop architecture, dynamic network topology, with both time and location varying spectrum availability [33]. Also CRAHNs have a functionality constraint of protecting the transmission of the licensed user or primary user (PU). The unique features of CRAHNs are listed below. Figure 2.3 provides an illustration of the CRAHN architecture and framework.

1. In CRAHNs, the spectrum opportunities (white spaces or holes) are distributed over a wide range of frequencies which vary in time and space

2. In traditional AHNs topology information and updates are easily sent as a beacon message over a single channel. However, CRAHNs are likely to have

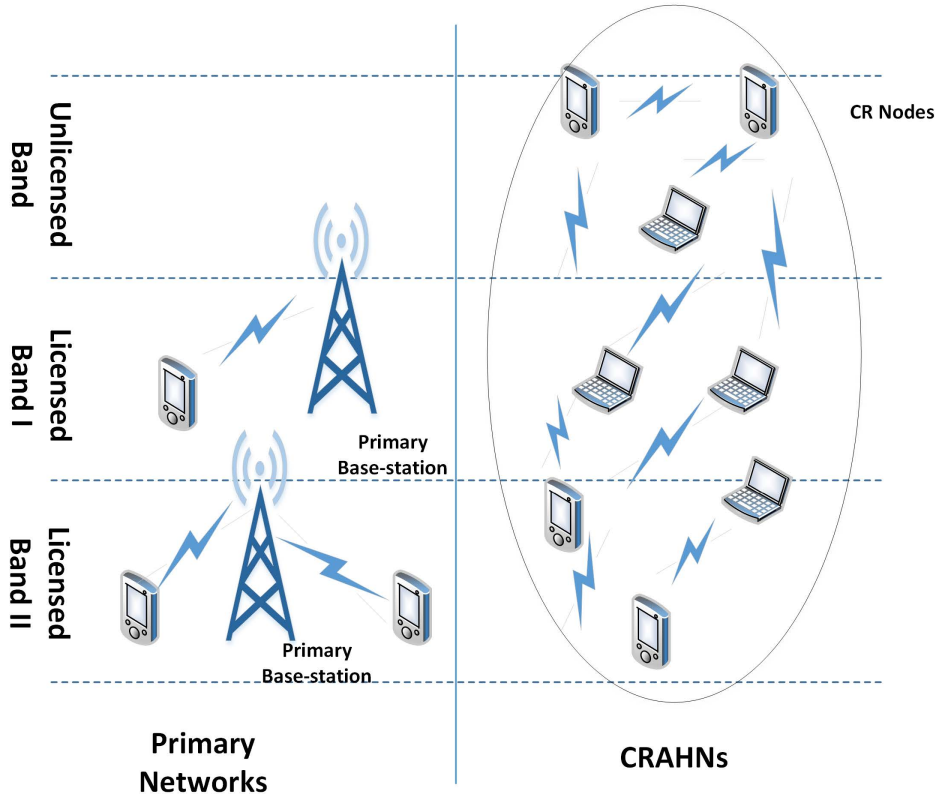

Figure 2.3: CR Adhoc Network Architecture [33]

incomplete topology information, since sending beacons over all the channels is not feasible.

3. Multi-hop/multi-spectrum transmission: The end-to-end route in CRAHN may consist of several hops with nodes having diverse spectrum set.

In a real sense, the CR network is assumed to be a stand-alone network and do not have direct communication with the PU network. Therefore, there is the need for a robust collaboration among nodes in the network, since the CR nodes decisions are based on local observations shared among themselves. In a bid to fully deploy the CRAHN, the four building block of CR mentioned in Section 2.2 must be addressed and integrated.

2.4 Spectrum Sensing in CR Technology

Spectrum sensing has been an area of strong research interest in recent literature. Several spectrum sensing techniques and strategies have been proposed in the literature. They include but not limited to matched filter, energy detection, wavelet based, cyclostationary detection techniques, cooperative and non-cooperative sensing strategies. However, it is noteworthy that in various texts; these techniques have been grouped into different forms while there are other techniques which are hybrids of the major sensing techniques.

In the SS task, the sampled received waveform $y(n)$ over a noisy channel is compared to two hypothesis H_0 and H_1. Let H_0 denote the hypothesis that the random waveform is only white Gaussian noise i.e

$$H_0 : y(n) = w(n) \tag{2.1}$$

where $w(n)$ for $n = 1, 2, \ldots$ are independent, zero mean, Gaussian random variables, with variance σ^2.

Similarly, let H_1 denote the hypothesis that the waveform $y[n]$ is the sum of white Gaussian noise $w[n]$ and a known, deterministic signal $s[n]$ [34], that is

$$H_1 : y(n) = s(n) + w(n) \tag{2.2}$$

The task is to decide in favour of H_0 and H_1 based on the measured sample $y[n]$. The performance of the spectrum sensing algorithm is mostly evaluated with the probability of false alarm, the probability of miss detection and the probability of detection. A plot of the probability of detection against the probability of false alarm

as the Signal to Noise Ratio (SNR) varies is termed Receiver Output Characteristic (ROC) curve.

The possible outcome that is relevant to evaluating the decision rule consists of the following four mutually exclusive and collectively exhaustive possibilities: H_i is true, and we declare H_j, where $i, j = 1, 2$. Considering the four possible outcomes, the two that represent errors are declaring H_0, when H_1 and declaring H_1, when H_0.
Thus, the error probability P_e averaged over all possible values of the measured random variable is given by [34]

$$P_e = \quad P(H_0', H_1') + P(H_1', H_0') = \quad p_0 P('H_1'|H_0) + p_1 P('H_0'|H_1), \tag{2.3}$$

where $P('H_1'|H_0)$ is referred to as the conditional probability of a false alarm, denoted by P_{FA}. Similarly $P('H_0'|H_1)$ represents the conditional probability of a miss detection, and simply denoted by P_M.

2.4.1 Matched Filter

Matched Filter technique involves correlating a known signal, in this case PU, with an unknown signal; that is the measured signal, to detect the presence of PU signal. This is the same as convolving the measured signal with a conjugated time-reversed version of the known PU sample. The correlated sum constitutes a linear operation on the measured signal, this is computed using an LTI (Linear, Time-Invariant) Filter, and the output is sampled at an appropriate time to form the correlation sum g, given below [34]

$$g = \sum_{k=-\infty}^{\infty} y[k]h[n-k] \tag{2.4}$$

For $y[n] = 0$ except for $1 \leq n \leq L$ and with $h[n]$ channel impulse response chosen as $s[-n]$, the filter output at $n = 0$ is

$$g = \sum_{k=1}^{L} y[k]h[n-k] \tag{2.5}$$

The filter impulse response is chosen as a time-reversed version of the target signal for $n = 1, 2, \ldots, L$ with $h[n] = 0$ elsewhere [34]. Therefore this filter is referred to as the matched filter for the target signal. Figure 2.4 is an illustration of matched filter detector:

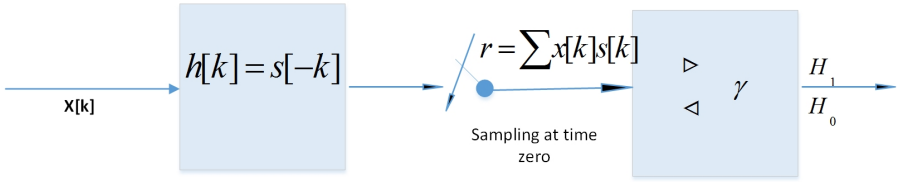

Figure 2.4: Matched Filter block diagram

MF is the fastest approach for spectrum sensing, however, the fact that prior knowledge of the primary user's signal is needed plagues the Matched Filter, therefore it is not suitable for optimal CR operation. Also Wang and Liu, in their work [35] observed that the performance of the Matched Filter largely depends on the number of signal samples, so that for low SNR the sample size increases, hence, an SNR wall always exist for the Matched Filter. Also, the complexity of its implementation and power consumption is rather high [36].

2.4.2 Energy Detector (ED)

The ED is the least computationally intensive and an easy to implement technique for spectrum sensing. Figure 2.5 is the functional block diagram of a simple ED. The ED, due to its simplicity, has several techniques for its realisation [4, 11, 18, 37].

These include Periodogram, Autoregressive (AR), Compressive (wavelet) Sensing and Multitaper-Singular Value Decomposition (MTM-SVD). In this section, a general description of the ED is presented. The received signal $r(t)$ is first filtered by a band-pass filter to select the channel of interest. Next, the detector computes the energy of the discrete time samples obtained from the A/D signal converter and compares against a predetermined threshold λ_e [38].

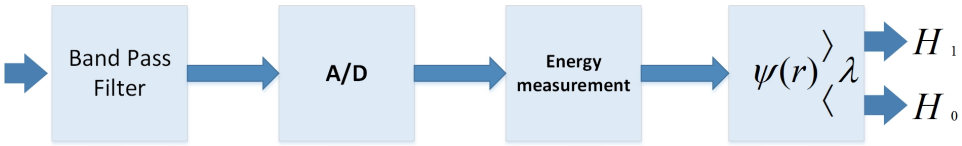

Figure 2.5: Energy Detector block diagram

The Neyman Pearson's (NP) test compares the log-likelihood ratio with a predetermined threshold $\lambda_e$as shown in equation 2.6 [39, 40].

$$\log\left(\frac{P(r_0, r_1, \ldots, r_(N-1)|H_1)}{P(r_0, r_1, \ldots, r_(N-1)|H_0)}\right) \gtrless_{H_0}^{H_1} \lambda_e, \tag{2.6}$$

where $P(r|H_1)$, $P(r|H_0)$ are the probability density function of H_1 and H_0 respectively. The ED does not have the prior knowledge of the PU signal to be detected; this is due to the presence of the AWGN. Therefore, the above equation can be approximated as

$$\Psi(r) = \sum_{n=0}^{N-1} |r[n]|^2 \gtrless_{H_0}^{H_1} \lambda_e, \tag{2.7}$$

here $\Psi(r)$is the measured energy and λ_e is the threshold, obtained from equation 2.8 [41, 42]

$$\lambda_e = F^{-1}(1 - P_{f-des}|U, \sigma_w^2), \tag{2.8}$$

and F^{-1} is an inverse gamma function, P_{f-des} represents the desired false alarm probability, U and σ_w^2 are the shaping and sizing parameters, and both depend on the sample size N and variance of the noise respectively [42].

For a large band, the number of sample N is τf_s, where τ is the sensing time and f_s is the sampling frequency. Assume the test statistic follows a normal distribution, then the mean μ_i and variance σ_i under the hypothesis H_i $(i \in 0, 1)$ are as shown in equation 2.9, 2.10, 2.11,2.12 [43, 44, 45].

$$\mu_0 = \sigma_n^2, \tag{2.9}$$

$$\sigma_0 = \frac{\sigma_n^2}{\sqrt{\tau f_s}}, \tag{2.10}$$

$$\mu_1 = \sigma_n^2 * (1 + \gamma), \tag{2.11}$$

$$\sigma_1 = \sigma_0^2 * \sqrt{(2\gamma + 1)}, \tag{2.12}$$

where γ is the signal to noise ratio (SNR).

The probability of detection and false alarm are given by equation 2.13 and 2.14 respectively.

$$P_d = Q(\frac{\lambda_e - \mu_1}{\sigma_1}), \tag{2.13}$$

The Q-function represented by $Q(x)$ is the complementary distribution function of the Gaussian function.

$$P_f a = Q(\frac{\lambda_e - \mu_0}{\sigma_0}). \tag{2.14}$$

Equation 2.13 and 2.14 may be simplified further as shown in 2.15 and 2.16 respectively

$$P_d = Q\left((\frac{\lambda_e}{\sigma_n^2} - \gamma - 1)\sqrt{\frac{\tau f_s}{2\gamma + 1}}\right), \tag{2.15}$$

$$P_f a = Q\left((\frac{\lambda_e}{\sigma_n^2} - 1)\sqrt{\tau f_s}\right). \tag{2.16}$$

2.4.3 Cyclostationary Feature Detection (CFD)

Modulated signals are usually integrated with sine wave carriers, pulse trains, hopping sequences and cyclic prefixes which introduce periodicity into the signal. Therefore, CFD detects and extracts features in the received waveform by analysing the spectral correlation function between the noise samples and signal samples. Note that noise is a stationary signal with no correlation while modulated signals are cyclostationary with spectral correlation, as a result of the in-built periodicity [46]. Figure 2.6 shows a modular implementation of the CFD.

A stochastic process X is wide-sense cyclostationary if and only if the mean, m_x, and the autocorrelation R_x are periodic as shown in equation 2.17 and 2.18;

$$m_x(t) = \mu(t + nT_0), \tag{2.17}$$

$$R_x(t, \tau) = R_x(t + nT_0, \tau + nT_0), \tag{2.18}$$

where T_0 is the period of the mean and autocorrelation, τ is the lag associated with the autocorrelation function, t is the time index, and n is an integer.

Fourier series representation of equation 2.18 is shown in equation 2.19 when considering a fixed τ.

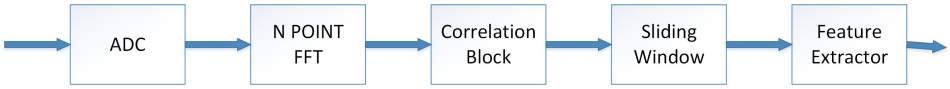

Figure 2.6: CFD block diagram

$$R_x(t,\tau) = \sum_{\alpha=-\infty}^{\infty} R_x^{\alpha}(\tau) e^{-2j\pi\alpha t}, \tag{2.19}$$

where $R_x^{\alpha}(\tau)$ represents the Fourier coefficient function given by equation 2.20

$$R_x^{\alpha}(\tau) = \frac{1}{T} \int_{-\frac{T}{2}}^{\frac{T}{2}} R_x(t,\tau) e^{-2j\pi\alpha t} dt, \tag{2.20}$$

The received signal is classified H_0 if the measured signal has no periodicity and H_1 if cyclostationary or periodic [47].

2.4.4 Wavelet Transform Method

Wavelets are families of functions $\Psi_{s,t}(x)$ generated from a single base wavelet $\Psi(x)$ by dilations and translations, and modelled as shown in 2.21

$$\Psi_{s,t}(x) = \frac{1}{\sqrt{|s|}} \Psi\left(\frac{x-t}{s}\right), \tag{2.21}$$

where s is the dilation parameter, and t is the translation parameter [48]. This set of wavelets were first introduced by Mallet *et al.* [49].

The dyadic wavelet transform is normally obtained by discretizing the scale variable s, and the resultant equation is shown in 2.22. The translation index k can take values from $(0, \pm 1, \pm 2, \dots)$ while j that is considered to be the decomposition level can take values from $1, 2, 3 \dots J$.

$$\Psi_{j,k}(x) = \frac{1}{\sqrt{|2^j|}} \Psi \left(\frac{x-k}{2^j} \right) \tag{2.22}$$

From the 2.22, we can obtain the discrete wavelet transform coefficient $W(j,k)$ of an arbitrary signal $f(x)$ as

$$W(j,k) = \int_{-\infty}^{\infty} f(x) \Psi_{j,k}(x) dx, \tag{2.23}$$

where $\Psi_{j,k}(x)$ denotes the set of wavelet function values.

We obtain the inverse wavelet transform from the coefficient $W(j,k)$ as

$$f(x) = \sum_{j=1}^{J} \sum_{k=1}^{K} \widetilde{\Psi}_{j,k}(x) W(j,k), \tag{2.24}$$

where $\widetilde{\Psi}_{j,k}(x)$ is the normalized dual basis function of $\Psi_{j,k}(x)$. The dyadic wavelet coefficient $W(j,k)$ are computed in a 2-D space of j and k such that $J = log_2 K$. Where J and K are the maximum numbers of scale of the decomposition and position of the original signal respectively. The key advantage of the wavelet transform is that, at different scale space decomposition, signal edges are positively correlated with the amplitude of $W(j,k)$ increasing or at worst remain constant. In contrary, noise is negatively correlated as we increase the scale j [48]. Using this technique, we detected PU signal in a low SNR ratio scenario. In chapter 3 we present a detail application of wavelet-based method.

2.4.5 Compressive Spectrum Sensing

In compressive spectrum sensing technique, the time-domain samples at individual CR receiver is compressed. To achieve this, a compressive sampling matrix S_c at each CR is utilised to collect a $K \times 1$ time-domain sample vector $x(n)$ from the measured signal $r(t)$ by the CR as follows,

$$x(n) = S_c r(n), \tag{2.25}$$

here $r(n)$ is an $M \times 1$ vector representing the discrete time values of $r(t)$ at the Nyquist sampling rate f_{Nyq}[50]. Therefore the average sample is $(K \div M) f_{Nyq}$ where $K \ll M$ is chosen to induce strong compression, however for accurate recovery of signal, in [51] and [52] K is chosen to be greater than the spectrum sparsity.

The compressed sample vector $x(n)$ is dependent on the high-resolution transmitted spectrum from the primary transmitter S_p as follows,

$$x(n) = S_c F_M^{-1} H_p S_p + S_c F_M^{-1} w_f, \tag{2.26}$$

here F_M is the M-point discrete Fourier transform (DFT) matrix, and H_p is the channel response matrix. Given the spectrum utilisation by PU is low, the unknown vector S_p is measured using the l-norm $\parallel S_p \parallel_l$, for $l \in [1, 2)$ as shown in equation 2.27

$$\min_{Sp} \parallel S_p \parallel_1 + \lambda \parallel x(n) - S_c F_M^{-1} H_p S_p \parallel_2^2, \tag{2.27}$$

where the $l_1 - norm$ minimization term enforces sparsity and is a positive scalar weighting coefficient balancing the bias-variance tradeoff [52] [53]. In the presence of measurement noise, the recovery is approximate, and the estimation error level

depends on the sampling matrix, the compression ratio and the signal sparsity order [50].

2.4.6 Subspace Spectrum Sensing

In subspace method, multiple receiver antennas are employed. The detection of PU signal is based on the fact that the PU signal is correlated while noise signal is spatially and temporally white[54]. The Subspace is similar to the Wavelet approach, Matched Filter and cyclostationary techniques that rely on correlation of features. However, in a Subspace-based detection method the signal feature is extracted from the specific structure of the sample covariance matrix.

Consider the sampled signal model in equations 2.1 and 2.2, let the sample covariance matrix of the received signal such that it characterises the subspace features be

$$\hat{R}_y = \frac{1}{N}\sum_{n=0}^{N-1} y[n]y^H[n], \tag{2.28}$$

here H is the channel state information. The test statistic for the subspace method can be obtained using eigenvalues, $\lambda_i, \forall i = 0, \ldots, L-1$. sorted in descending order of the magnitude as follows,

$$\Psi(r) = \frac{max_i \lambda_i}{min_i \lambda_i} \gtrless_{H_0}^{H_1} \lambda_e, \tag{2.29}$$

The above maximum-minimum eigenvalue (MME) detection method for subspace technique was proposed by Zeng and Liang in [55]. A decision threshold is derived with the knowledge of the distribution of $\Psi(r)$ given that the false-alarm probability is fixed. Alternatively, the covariance based test statistic may be employed as in

[56], here the asymptotic distribution of the ratio was obtained for a selected decision threshold.

2.4.7 Machine Learning Technique in Spectrum Sensing

Machine learning (ML) techniques are often used for pattern classification. In ML a featured vector is extracted from a pattern and is fed into a classifier which then categorise the pattern into class. However in the context of CR this featured vector is an energy vector, with each component of the vector an estimate of the energy level measured by the CR [57]. ML may be considered as a sensing strategy than technique. It still relies on the conventional sensing technique to estimate the energy vector. Figure 2.7 describes the machine learning approach, before channel classification, the classifier is first trained with the training feature vector. The training is done according to the classification algorithm being implemented by the classifier. A classification algorithm can be categorised as unsupervised learning, these include K-means clustering and Gaussian mixture model (GMM) or supervised learning, examples are support vector machine (SVM) and K-nearest neighbour (KNN)[58, 59]

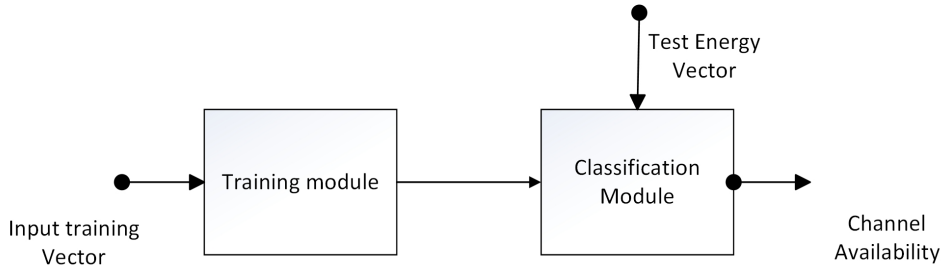

Figure 2.7: Machine Learning in Spectrum Sensing

2.4.8 Other sensing methods

There are several other spectrum sensing algorithms in the literature. However, the conventional spectrum sensing techniques have been discussed. Other spectrum sensing algorithms are variant of the above techniques, which party rely on the discussed conventional techniques but may differ regarding areas of application. These other algorithms include; radio identification based sensing, cooperative spectrum sensing, covariance based detection, entropy estimation, detection based on Bayesian criterion, interference-based detection, eigen value-based spectrum sensing, multitaper spectral estimation, and time-frequency analysis [60, 61, 36, 62, 63, 64, 65, 66, 67, 68, 69]

2.4.9 Assessment of the major spectrum-sensing techniques

The various spectrum sensing techniques present innate advantages and disadvantages. Therefore, in selecting any spectrum sensing technique for CRAHN, we must put into consideration the CRAHN's limitations. This network is because CRAHNs exhibit dynamic network topology as such there is the need to have a fast spectrum-sensing algorithm to adapt to the changing network topology. However, a direct relationship exists between sensing speed, accuracy and SNR [3]. The relationship is shown in equation 2.30

$$A(\gamma) \propto T_s. \tag{2.30}$$

Equation 2.30 shows that as sensing time is reduced, the accuracy which is a function of SNR (γ), also reduces. The ED although simple and fast regarding sensing time when signal strength is close to the noise floor, the performance of the Receiver Output Characteristics (ROC) deteriorates. The CFD, the MF and the Wavelet transform

method perform better than the ED regarding the ROC in low SNR condition but require longer sensing time [70, 71].

Table 2.1 shows some spectrum sensing techniques highlighted in this chapter along with its pros and cons. Some factors to consider in the choice of spectrum sensing technique include the desired accuracy, the sensing duration, network requirements and the computational complexity. Fig. 2.8 presents a normalised comparison of some spectrum sensing techniques regarding their accuracies and complexities [36]. The Wavelet based spectrum sensing technique present a higher accuracy with reasonable lesser complexity when compared with the Cyclostationary and Matched Filter techniques.

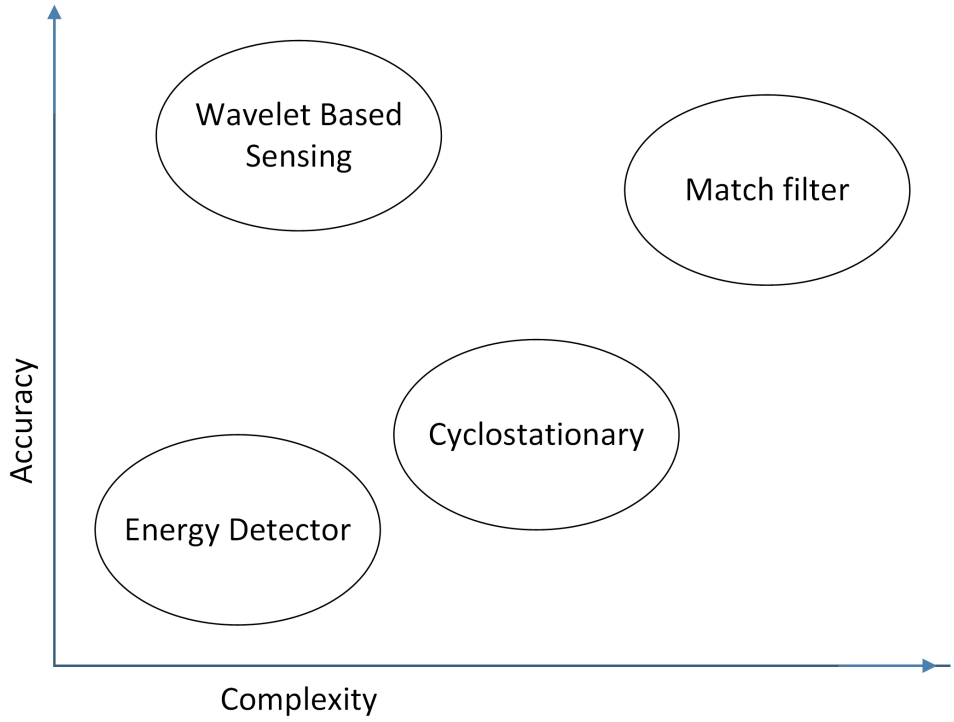

Figure 2.8: Main sensing methods' sensing accuracies and complexities [36]

In chapter 3, an Adaptive Wavelet-Based Scale Space Filter Approach for SS to compliment the ED SS technique in CRAHN was presented. This approach performed well with higher accuracy at low SNR.

Table 2.1: Comparison of some spectrum sensing techniques

Spectrum Sensing Technique	**Advantages**	**Disadvantages**
Matched Filter Detection	Fastest Sensing time. Best for white Gaussian noise model.	High complexity, prior knowledge of PU signal is required. In addition MF requires synchronization with PU.
Energy Detection	Low complexity. Easy and simple to deploy.	Performance is highly dependent on Noise Variance. Poor performance in low SNR.
Cyclostationary F̃eature Detection.	Resilient to Variations in the noise level. Good performance at low SNR [72].	High complexity. Computationally intensive. Longer Sensing time[71].
Wavelet Based S̃pectrum Sensing.	Good performance at low SNR. Resilient to Variations in the noise level[70].	Quite computationally intensive compared with the ED, Longer Sensing time.

2.5 Threshold Estimation for Spectrum Sensing

In spectrum sensing, threshold estimation is an essential component. Estimated threshold values are used to classify spectrum occupancy. Also, the performance of the Receiver Operating Characteristics (ROC) is dependent on the threshold values. Different threshold estimation techniques can be found in literature and are broadly classified as either fixed threshold or autonomous and adaptive threshold estimation technique. In spectrum sensing, traditional threshold approach is fixed. Some examples of fixed threshold techniques are; empirical analysis of spectrum measurements [73], receiver noise characteristics thresholding [74], P-tile based threshold technique [75] and histogram analysis (Laplacian Threshold) technique [76]. The downfall of this approach is that the system requires a priori knowledge of the

noise power and spectrum activity. Also, this technique lacks dynamism and is not adaptive to the changing noise floor.

The adaptive and autonomous threshold estimation techniques can estimate the value of the threshold from a given set of spectrum measurements without any need for prior knowledge of the noise level or spectrum occupancy [45]. These techniques introduce dynamism and automation since the value of the decision threshold varies adaptively and exclusively based on the interaction with the time varying radio environment. Some of the examples of the adaptive and autonomous threshold techniques which are popular in literature include; Maximum Normal Fit (MNF) [77], Principal Component Analysis (PCA) [78], Otsu's algorithm [79], Recursive One-Sided Hypothesis Testing (ROHT) [80].

Otsu's method is a popular thresholding method that assumes the image contains two classes of pixels - foreground and background and has a bi-modal histogram. It then attempts to minimise their combined spread (intra-class variance). In this work, we adopt this image processing technique to signal processing. The Otsu is considered a simple algorithm with an order O(N) complexity; it is truly an adaptive thresholding method as it splits the data into a grid of cells and then applies a simple thresholding method on each cell treating it as separate data.

An alternative approach to finding the local threshold is to statistically examine the intensity values of the local neighbourhood of each data. The threshold is different for each data and calculated from its local neighbourhood but is a more complex approach. Other techniques employ the variational Minimax Optimization approach. These are iterative method, based on optimising an energy function that is a nonlinear combination of two components. One component aims to calculate the threshold based on the position of strongest data changes in the image. The other component

aims to smooth the threshold at the (object) border areas, but requires a careful choice of the number of iterations and rather complex to implement.

2.6 Spectrum Access/Coordination

The core function of spectrum access/coordination in CRAHN is to control and avoid/prevent any interference to PUs as well as collision avoidance amongst SUs' traffic or signalling. This function is implemented as a protocol in the Medium Access Control (MAC) layer. The CR MAC acts as a link between the CR physical layer and the CR network layer. It uses spectrum sensing results obtained from the CR physical layer to characterise the channels and decide which set of channels to use, when and how it can be accessed [21, 81, 26]. In summary, the CR MAC must support the following functions.

1. *Interference control and avoidance for PUs*: There are two modes for spectrum sharing between SUs and PUs. The overlay and the underlay mode. In the overlay sharing mode, the SUs must vacate the channel as soon as the PUs return. Whereas in the underlay, SUs use the same channel with PUs as long as the interference from SUs to PUs is no more than the predefined threshold [21, 26]. This underlay mode uses the ultra wideband technology (UWB). In this work, the overlay mode is assumed.

2. *Collision avoidance amongst SUs*: Because different SUs may coexist, collisions may happen if they simultaneously move to and use the same spectrum band according to their spectrum-sensing results. Thus, the CR MAC should control the spectrum access of different SUs to avoid collisions [21, 26]. This can be handled using control signalling.

In CRAHNs, each CR senses the spectrum environment to determine spectrum availability based on local observations. Consequently, there is a need for an efficient cooperation scheme for spectrum opportunities exchange. A common cooperative scheme is forming clusters to share the sensing information locally. This scheme selects a single node to coordinate spectrum sensing information and channel access among the participating CR nodes. In [82], Chowdhury and Akyildiz proposed a cluster head formation for the mesh network. Here, the mesh clients send their individual sensing results to the mesh router. The mesh router acts as the central coordination entity. But, CRAHNs do not have the central network entity, this cooperation is implemented in a distributed manner [33].

Consider a scenario when a CR user (SU) detects the arrival of the PU, it should notify the entire CRs in the CRAHN. To ensure this cooperation, a reliable control channel (CC) is needed for exchanging sensing information and control signals. CC facilitates a variety of operations from a transmitter-receiver handshake, neighbour discovery, channel access negotiation, topology change and routing information updates, to the cooperation among CR users [24]. Therefore, in this thesis, the emphasis is laid on the design of a robust CC. The CC design for neighbourhood discovery and reliable information exchange are critical issues in implementing CRAHNs.

2.7 Classification of Common Control Channel (CCC)

To improve spectrum utilisation efficiency, researchers alike have agreed on a need for a common control channel design for CRAHN. Several control channel schemes exist in literature, such as sequence-based, group-based, dedicated, and ultra-wideband schemes [24]. Noteworthy is that in several works, the use of different taxonomies for

CCC classifications has been observed. For instance, in [83, 84, 85] the CCC design schemes are classified as dedicated control channel, common hopping, split phase, and multiple rendezvous control channels (MRCC). However, in [86, 87], the CCC designs are classified as group/cluster-based, sequence-based, and dedicated CCC. For simplicity, the taxonomy in [33, 86, 24, 87] as shown in Fig. 2.9 is observed in this work.

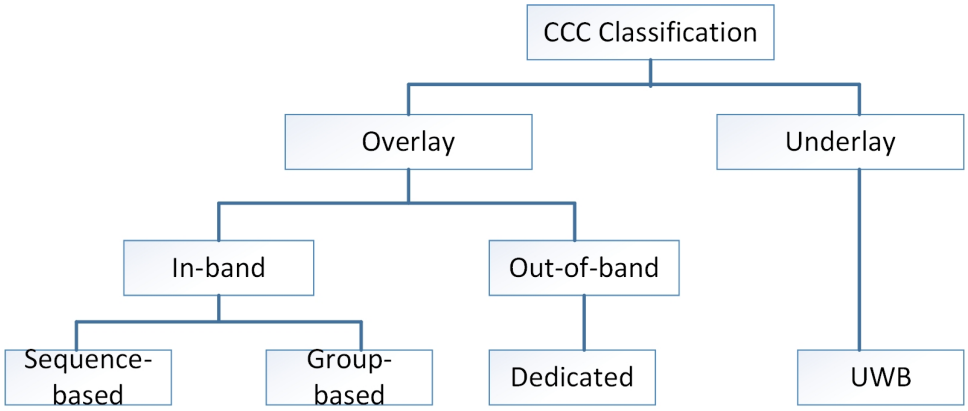

Figure 2.9: CCC Classification

The CCC designs are broadly classified as either Overlay or Underlay. In the Overlay CCC designs the control channel is vacated on arrival of the PU and must re-establish another CCC, but for underlay, the PU signal and the control signal of the CR are transmitted on the same channel using the spread spectrum technique. The control signal is transmitted at low power below the interference temperature using UWB technology. However of specific interest to this work is the overlay CCC design which is further classified as in-band and out-of-band. For in-band, the CCCs are shared by data channels while the CCCs for out-of-band schemes utilises dedicated channels. The dedicated (out-of-band) control channel is exposed to control channel jamming, coverage limitations and it is not always robust to PU activities. To this day the most favoured solution is the implementation of in-band (dynamic) CCC (DCCC) for CRAHN[24, 88].

2.8 Common Control Channel Design Schemes

In this section, some of the notable control channel design schemes will be presented:

2.8.1 Sequence-based CCC design

In sequence-based CC design scheme, a hopping sequence is generated. This can be pseudo-random [89], permutation [90], adaptive [91], modular clock [92] or quorum-based sequence[93]. This scheme allows for a dynamic control channel selection. This CC design diversifies the control channel allocation over different bands. This minimises the impact of PU activities. A review of these approaches is presented in chapter 5.

2.8.2 Group-based CCC design

In Group-based CCC design, the Control channel is designated to the channel that is common and available to all CR users in a closed group. The Group-based CCC design is achievable because CR users usually observe similar spectrum availability when in proximity [94]. This scenario of similar spectrum availability is called symmetry. In this case, CR users that use a common channel as the CCC are grouped to a local area. The group-based CCC designs allow control message broadcast within the group. The challenge with this approach is evident when inter-group communication is required. In this case, a need arises for a universal CCC.

2.8.3 Dedicated CCC design

Dedicated CCC are fixed in predetermined licensed or unlicensed bands. Although this design scheme is easy to deploy with little over-head and signalling cost, it is

vulnerable to control channel saturation and security attacks.It also defeats the goal of dynamic spectrum access. Popular dedicated CCC design in literature are OSA MAC [95], OS MAC [96], Opportunistic MAC [97, 98], DOSS MAC [99] and CREAM MAC [100].

2.9 Orthogonal Frequency Division Multiplexing (OFDM)

OFDM is a wideband digital communication technology. In OFDM, Frequency Division Multiplexing (FDM) mechanism is employed. The single wideband signal is divided into a large set of narrowband sub-carriers in such a way that, all of the sub-carriers are orthogonal to each other and evenly spaced. OFDM involves bundling evenly spaced multiple sub-carriers together and transmitting separately over the transmission media.

2.10 Evolution Algorithm (EA)

Evolution Algorithm is an Artificial intelligence technique that involves evolutionary computation. EA is a generic population-based metaheuristic optimization algorithm. EA uses mechanisms inspired by biological concepts, such as reproduction, social behaviour, mutation, recombination, selection, pheromone deposit, swarm flocks, frog leaping e.t.c. to perform a stochastic search for an optimal or near optimal solution. Among the popular EAs are Genetic Algorithm, Memetic Algorithm, Particle Swarm, Ant Colony and Shuffled Frog leaping[101, 102, 103, 104]. The EAs in some instance do not completely address well, all optimisation problems. This is because EAs has specific representational components and mechanism. For instance,

in Genetic Algorithm, it is cross over and schematics whereas in ACO, it's edge-based construction and edge weights. Rather than trying to fit a problem to all the EAs, systems are first analysed on the problem at hand, identify key components, and then try to match these components to a suitable EA. In this thesis, the ACO specific representation components such as pheromone updates, cost computation and transition probability are customised to solve the Common Control (CC) channel selection problem in Chapter 4.

2.10.1 Ant Colony Systems

The Ant Colony Optimization (ACO) technique is based on the behaviour of real ants. Real ants deposit pheromone on tracks and through a complex sensing algorithm seek the shortest route between their nest and a food source [105]. The application of ACO can be seen in many optimization problems such as the 2D-HP protein folding [106], scheduling [107], assembly line balancing [108], sequential ordering [109], probabilistic Travelling Salesman Problem (TSP) [110], DNA sequencing [111], and proteinligand docking [105] [112]. In this work, the adoption of ACO in solving the problem encountered while searching for a common control channel in CRAHN was proposed. The ACO technique imitates the behaviour of real ants in several ways:

1. Artificial ants deposit pheromone trails on the nodes of quality paths. This pheromone deposited is proportional to the quality of the path.

2. Artificial ants construct solutions by moving through the construction graph, and they (artificial ants k)choose their path with respect to probabilities $P_{i,j}^{k}(t)$, which depend on the pheromone trails previously deposited as shown in equation 2.31.

3. Artificial pheromone trails deposited previously decrease sufficiently at each iteration. Therefore simulating the slowly evaporative pheromone trail phenomena observed in real ants as shown in equation 2.32.

The state-transition probability rule guides ant movement through a stochastic local decision policy that essentially depends on both pheromone information and heuristic information.

$$Pr_{i,j}^{k}(t) = \begin{cases} \dfrac{\tau_{i,j}^{\alpha}(t) * \eta_{i,j}^{\beta}}{\sum_{k=1}^{N} \tau_{i,j}^{\alpha}(t) * \eta_{i,j}^{\beta}} & j \in N_i^k \\ 0 & otherwise \end{cases} \tag{2.31}$$

where: $P_{ij}^{k}(t)$ is the probability of the k^{th} ant to move from node i to node j at the t^{th} iteration/time step. N_i^k is the set of nodes in the neighbourhood of the kth ant in the ith node. $\tau_{i,j}^{\alpha}(t)$ is the pheromone amount on the arc connecting node i and node j, weighted by α(an application-dependant constant) $\eta_{i,j}^{\beta}$ is the heuristic value of the arc connecting node i and node j, weighted by β(an application-dependant constant).

$$\tau_{i,j} = (1 - \rho)\tau_{i,j} + \rho\Delta\tau_{i,j} \tag{2.32}$$

where ρ is a variable $(0 < \rho < 1)$ that controls the evaporation rate of the local pheromone which is deposited on channels thereby enabling the system to eliminate channels m that are bad solutions. $\Delta\tau_{m,n}$ denotes the pheromone trail deposited on channel m of node n.

2.10.2 Other Evolution Algorithms

Several other evolution algorithms are found in the literature. They include but not limited to the following; Genetic Algorithm, Particle Swarm Optimization, Memetic algorithm and Shuffled Frog Leaping, just to mention a few. In this thesis, the Ant

Colony was adopted due to its simplicity and quick convergence. However, this section briefly discusses other EAs in literature.

Genetic algorithm (GA) is a method for solving both constrained and unconstrained optimisation problems based on a natural selection process that mimics biological evolution. The algorithm repeatedly modifies a population of individual solutions[113]. At each step, the genetic algorithm randomly selects individuals from the current population and uses them as parents to produce the children for the next generation. Over successive generations, the population "evolves" toward an optimal solution. This innovative technique, the GA, unlike the ACO, generates a sequence of solutions that approaches the optimal solution over several iterations. It selects the next solution using random number generators, further increasing complexity and simulation time. GAs finds application in solving problems that are not well suited for standard optimisation algorithms, including problems in which the objective function is discontinuous, non-differentiable, stochastic, or highly non-linear. The pseudo code for GA can be found in [104].

Memetic algorithm (MA): In an attempt to improve on processing time and the quality of the solution, other EAs have evolved over the past decade. The Memetic algorithm (MA) inspired by Dawkin's notion of a meme, provides improved convergence time [114]. Memetic algorithm is an extension of the traditional genetic algorithm[115]. In addition to the features of a GA, It uses a local search technique to reduce the likelihood of the premature convergence. In MAs, the elements that form a chromosome are referred to as memes and not genes as in GAs. The unique aspect of the MAs algorithm is that all chromosomes and offsprings are allowed to gain some experience, through a local search, before being involved in the evolutionary process [116]. As such, the term MAs is used to describe GAs that heavily use local search [117].

Particle swarm optimisation: Particle swarm optimisation (PSO) is a population-based stochastic optimisation technique developed by Eberhart and Kennedy in 1995, inspired by social behaviour of bird flocking or fish schooling[118]. In PSO, solutions are found by birds flocking. Each bird referred to as particle is analogous to a chromosome (population member) in GAs. As opposed to GAs, the evolutionary process in the PSO does not create new birds from parent ones. Rather, the birds in the population only evolve their social behaviour by adjusting their velocity and position toward a destination [119, 120]. The PSO is a combination of both local search (learning from its experience) and global search technique (learning from the flock). Each bird/particle looks in a specific direction and while exchanging information identify birds with the best position. Thereby, speeding to the new position in accordance with its current position. This process in an iterative process until the destination is reached.

Shuffled Frog Leaping Algorithm (SFLA) The SFLA was developed only recently by Muzaffar Eusuff and Kevin Lansey. They simply observed, imitated and modelled the behaviour of frogs searching for food laid on discrete stones randomly located in a pond [121, 122]. SFLA, in essence, combines the benefits of the genetic-based MAs and the social behavior-based PSO algorithms. In the SFL, the population consists of a set of frogs referred to as solutions that are partitioned into subsets referred to as memeplexes. The different memeplexes are considered as different cultures of frogs, each performing a local search. Within each memeplex, the individual virtual frogs hold ideas, that can be influenced by the ideas of other virtual frogs, and evolve through a process of memetic evolution. After a defined number of memetic evolution steps, ideas are passed among memeplexes in a shuffling process [123]. The algorithm contains elements of local search and global information exchange. In each memeplex, the local search is completed using a particle swarm optimisation method adapted for discrete problems but emphasising a local search.

Whereas to ensure global exploration, the virtual frogs are periodically shuffled and reorganised into new memeplexes in a technique similar to that used in the shuffled complex evolution algorithm.

2.11 Chapter Summary

In this chapter, we discussed the Cognitive Radio Technology, as a technology that enables dynamic spectrum access. We further gave an insight into the Cognitive Radio Ad Hoc Network (CRAHN), which forms our network of interest, pointing out its advantages and peculiarities. We then presented an overview of the major spectrum sensing techniques, capping the section with an appraisal of the various spectrum sensing techniques mentioned above. Furthermore, we discussed some threshold techniques in literature, including the Otsu's adaptive threshold technique of interest. After that, we presented spectrum coordination and access as a vital part of CRAHN and also introduced readers to the concept of spectrum coordination and the various control channels design schemes. The essence is to provide the reader, an insight into the CR modules, namely spectrum sensing and access modules, that we addressed in this thesis. We rounded up the background to the study with a concise introduction to the Evolution Algorithms including the ant colony system model. Therefore, this chapter sets the foundation for the development of the adaptive and autonomous MAC protocol for CRAHN. The next chapter discusses the development of the Adaptive Wavelet-based Scale Space Filtering Algorithm for Spectrum Sensing in Cognitive Radio.

Chapter 3

Development of an Adaptive Wavelet-based Scale Space Filtering Algorithm for Spectrum Sensing*

3.1 Introduction

The wireless communication industry is now faced with the challenge of spectrum scarcity. This is due to the recent increase in the development and deployment of new wireless technologies [125, 126]. The implication of spectrum scarcity is that the current user perceived Quality of Service (QoS) will slowly degrade in the nearest future resulting in increased user dissatisfaction and revenue loss for the industry.

Towards addressing this problem, Cognitive Radio (CR) has been proposed [38]. This proposal is based on research findings showing that allocated spectrum (to Licensed

*The contents of this chapter are from Ohize *et.al.* [124]

Users (LUs)) are widely underutilised in different geographical areas at different times. Towards exploiting these underutilised bands, CRs are expected to sense their spectral environment (spectrum sensing) and to optimally adjust their transmission parameters for the purpose of interference-free communication.

Consequently, SS is a fundamental function in CR, and it is currently receiving quite a lot of attention from CR researchers. However, one major problem in SS focuses on how to improve detection performance in low SNR conditions (typically less than 0dB). The popularly proposed ED fails in this low SNR region. Thus, despite its appealing features such as fast sensing, low complexity and ease of deployment, it is not yet deployed (for poor performance in low SNR region).

In an attempt to improve detection in the low SNR region, this thesis developed and investigated the novel application of the Wavelet Transform (WT) and the Otsu's multi-threshold algorithm in constructing the AWSSF. In the original WSSF, when the spectrum is sensed, the WSSF algorithm computes the wavelet coefficients associated with the signal. It then directly multiplies the wavelet coefficients across different scales, during which the noise samples diminish, while the signal components gain prominence due to their inherent correlation. However, the WSSF algorithm, uses a static threshold approach, thus leading to the need for manual adjustments whenever the input data changes. Therefore, whenever the dataset changes in a sensing period, the algorithm will perform poorly due to the inability of the threshold to adapt.

Consequently, in this thesis, an integration of the Otsu's multi-threshold algorithm was proposed. Otsu's multi-threshold algorithm was adapted from its use in Image Processing for use in the AWSSF in CR. To the best of the authors knowledge, this adaptation has never been done, as such; this novel construction of the AWSSF has led to an improved performance in low SNR region for SS. For demonstration purpose,

the performance comparison with the ED and other Wavelet based techniques is provided, and it is shown that the proposed AWSSF will be a great potential for CR deployment.

The rest of the Chapter is organised as follows: We discuss the relevant literature sources in Section 3.2; this is followed by an overview of WSSF and Otsu's algorithm in Section 3.3. The proposed AWSSF is presented in Section 3.4. The results and the discussion can be seen in Section 3.5; while the conclusions are drawn in Section 3.6.

3.2 Brief Review of Related Works

Wavelet Transform (WT) has been widely used in CR [127, 128, 129, 130, 131]. One early work was that of Tian and Giannakis [128], who proposed and applied WT in a fashion similar to what is called the WSSF algorithm. However, it is noted that the WSSF had already been proposed by Xu *et al.* in [132]. But in [128], Tian *et al.*, established the necessary mathematical theories that govern how WSSF works. They applied their approach to a test signal in CR and showed how effective the WSSF could be. However, their approach depended on a manual threshold method to classify the wavelet coefficients at different scales towards signal detection. This led to visual analysis of their results, which might not be realistic for automation purpose. Similarly, Xu *et al.*, [132], who were the first to propose the direct multiplication of scale levels in WSSF, also depended on manual thresholding to analyse their WSSF results, though their application was not for CR purpose.

On the other hand, the concept of combining WT with Adaptive Threshold Techniques (ATT) for SS in CR is a recent discussion in the literature. Wang *et al.*, [127] recently proposed an ATT algorithm for the Discrete Wavelet Packet

Transformation (DWPT) based Energy Detector (ED). In their work, the DWPT-ED first determined the level of scale decomposition and then a proposed adaptive threshold was used for classification in both the DWPT-ED and the Welch ED methods. Their adaptive threshold was implemented by varying the threshold influence ratio for a targeted probability of detection, or probability of false alarm. While the authors indicated the use of DWPT, they, however, failed to provide the needed details for its operation. Most importantly, there were certain limitations with Wang's ATT. The limitations include, the need for apriori knowledge of the primary user energy [127], (pp. 360), the dependence on an initial fixed threshold (manual), which may not be known in reality [127], (pp. 361), and the need to optimize the energy parameter, which might be data specific [127], (pp.360). Therefore, their approach may not be optimal.

In [129], Divakaran *et al.* developed a wavelet approach for spectrum sensing in CR and analysed the importance of selecting appropriate wavelet schemes. Authors also compared the muti-scale sum and the multi-scale product techniques in the wavelet transform, and their results showed that the multi-scale sum performed better than the multi-scale product. Similarly, their technique depended on manual thresholding and visual analysis of the output towards declaring free bands. Other works that used WT for CR purpose can be seen in [130] and [131].

Essentially, all the reviewed works (to the best of the author's knowledge) were limited in certain dimensions, such as, their dependence on manual threshold, which can under-perform if the dataset changes; and for those that used ATT, they needed prior knowledge of the primary user signal, which is unrealistic. Also, their ATT depended on manual threshold at some point in their operational process with its limitation already mentioned.

Thus, to address these limitations, while improving on SS performance in low SNR region, a novel adaptation of Otsu's threshold algorithm into WSSF to develop a new Adaptive Wavelet-based Scale Space Filter (AWSSF) algorithm was proposed. In addition, the WSSF was enhanced by introducing a new mechanism for autonomous identification of signal boundaries in the wavelet coefficients, as well as the use of peak-finding algorithm. These improvements are shown in this chapter.

3.3 Wavelet-based Scale Space Filter and Otsu Threshold

In this section, a background on the WSSF algorithm is provided, along with how the Otsu's threshold algorithm was adapted. The focus is to establish the basic models used in these algorithms, and to lay a foundation for their use in the extension (in Section 3.4).

3.3.1 Wavelet-Based Scale Space Filter Algorithm

Wavelets are families of functions $\Psi_{s,t}(x)$ generated from a single base wavelet $\Psi(x)$ by dilations and translations, and modelled as

$$\Psi_{s,t}(x) = \frac{1}{\sqrt{|s|}}\Psi\left(\frac{x-t}{s}\right), \tag{3.1}$$

where s is the dilation parameter and t is the translation parameter. This set of wavelets was first introduced by Mallat *et al.* [49].

The dyadic wavelet transform is normally obtained by discretizing the scale variable and the resultant equation is shown in 3.2. Note that the s and t parameters in 3.1

have been substituted by 2^j and a translation index k respectively. The translation index can take values from $(0, \pm 1, \pm 2, \dots)$ while j that is considered to be the decomposition level can take values from $1, 2, 3 \dots J$.

$$\Psi_{j,k}(x) = \frac{1}{\sqrt{|2^j|}} \Psi \left(\frac{x-k}{2^j} \right), \tag{3.2}$$

Equations 3.1 and 3.2 form the basis for the wavelet transform theory, and to proceed into its use in WSSF, let us henceforth consider the WT coefficients as $W(j,k)$ of the signal $f(x)$. Here $f(x)$ is the Power Spectral Density (PSD) of the measured signal $y(n)$. These coefficients can be computed by using 3.3, [48].

$$W(j,k) = \int_{-\infty}^{\infty} f(x) \Psi_{j,k}(x) dx. \tag{3.3}$$

Here, $\Psi_{j,k}(x)$ denotes the set of wavelet function values. Typically, the signal portion in noise can be isolated during the decomposition process as the scale factor j increases. This is achievable because the amplitude of the wavelet coefficients either increases or remains the same; as the signal edges become positively correlated; while noise reduces because it is poorly correlated.

The computed wavelet transform coefficients are then used for developing a scale space filtering algorithm as presented in [132]. The algorithm uses the direct multiplication of wavelet coefficients at adjacent scales to achieve a seemingly correlated output as follows

$$\Omega_j(j,k) = \prod_{i=0}^{J-1} W(j+i,k), \tag{3.4}$$

where Ω denotes the spatial correlation function, J is the number of multiplication scales, and $W(j+i,k)$ is the $(j+i)th$ wavelet coefficient at the K^{th} scale. Equation 3.4 is used to identify and isolate noise from the signal buried within. In [48, 132] the

scale space algorithm, Ω is obtained from the multiplication of adjacent scales. For example, the direct product of the coefficients at the scale j and at scale j + 1 (two levels multiplication) is

$$\Omega_2(j,k) = W(j,k)W(j+i,k). \tag{3.5}$$

The amplitudes of these coefficients increase from scale j to scale j + *1*, so that a comparison of *W(j, k)* and $\Omega_2(j,k)$ will show the enhancement of the modulus maxima of the signal, while at the same time, resulting in the suppression of the noise modulus maxima. To extract the desired signal coefficients, different rescaling schemes for different scales are performed iteratively.

In the rescaling scheme as described in [48], the correlation function $\Omega_2(j,k)$ is rescaled to *W(j, k)*. At small scales ($j < G$) (Here, G is the upper limit of small scales), it is necessary to extract the modulus maxima which correspond to the signals most important features. If we let

$$j\Omega(j) = \max_{1 \ll k \ll K} \mid \Omega_2(j,k) \mid \tag{3.6}$$

and

$$\Omega_2(j,\tau) = j\Omega(j). \tag{3.7}$$

then

$$jW(j) = \mid W(j,\tau) \mid, 1 \ll \tau \ll K, \tag{3.8}$$

A new scale is then obtained as derived in [48, 49, 133]

$$\tilde{\Omega}_2(j,k) = \Omega_2(j,k)\left(\frac{jW(j)}{j\Omega(j)}\right). \tag{3.9}$$

However, at large scales, the signal power corresponds to the low-frequency band with low noise power. Therefore, different power rescaling method is applied. That is, at large scale $j > G$, the scale power is given as

$$p\Omega(j) = \sum_{k=1}^{k} [\Omega_2(j,k)]^2 \tag{3.10}$$

$$pW(j) = \sum_{k=1}^{k} [W(j,k)]^2, \tag{3.11}$$

Equation 3.10 and 3.11 combine to give the rescale in 3.12,

$$\tilde{\Omega}_2(j,k) = \Omega_2(j,k)\sqrt{\frac{pW(j)}{p\Omega(j)}}. \tag{3.12}$$

Equation 3.9 and 3.12 indicate different rescaling function for small and large scales respectively. At all scale points, the rescaled value $\Omega_2(j,k)$ is compared to the coefficients $W(j,k)$. The algorithm uses the strength of these correlated features to discriminate between the signal features and the noisy features.

In principle, the scale space filter's first task is to rescale $\Omega_2(j,k)$ to $W(j,k))$ and then compare the value of the new scale $\tilde{\Omega}_2(j,k)$ to that of $W(j,k)$. The value of *W(j, k)* at the scale points *(j,k)* corresponds to the signal component if $|\Omega_2(j,k)| \geq |W(j,k)|$. This edge position and its corresponding value $W(j,k)$ are stored. Suppose that $\tilde{W}(j,k)$ denote the retained value at point *(j,k)*. This represents the important features of the signal and it is retained.

A brief summary of the algorithm is as shown in algorithm 1

Algorithm 1 Wavelet-Based Scale Space Filter

Input: Obtain the Power Spectral Density (PSD) from the measured signal $y(n)$. domain)

The set of wavelet coefficients at each scale is computed for the input PSD as $W(j,k)$ using equation 3.3.

The power of the correlated signal data $\Omega_2(j,k)$ at each scale is rescaled to the wavelet coefficient at that scale $W(j,k)$ using either equation 3.9 or 3.12.

An edge is identified, if the new absolute value of $\Omega_2(j,k)$ is greater than or equal to the absolute value of $W(j,k)$, when compared at the scale points (j,k). The edge position and its corresponding $W(j,k)$ value are saved.

Extracts all identified edges from $\Omega_2(j,k)$ and $W(j,k)$. After extracting the first round of edges at position (j,k), the remaining data points in $\Omega_2(j,k)$ and $W(j,k)$ are denoted as $\Omega_2'(j,k)$ and $W'(j,k)$ and then compared with their absolute values.

The next edge in the noise corrupted signal is extracted from $W(j,k)$ and $\Omega_2(j,k)$ by rescaling the power of $\Omega_2'(j,k)$ to that of $W(j,k)'$ and then comparing their absolute values.

This process of power normalisation, data value comparison and edge information extractions is iterated many times until the power of the un-extracted data points in $W(j,k)$ at the scale points (j,k) is approximately equal.

The final filtered signal is saved in $W_{new}(j,k)$

Output: Obtain the detected PU signal, $W_{new}(j,k)$

3.3.2 Otsu Threshold Algorithm

A commonly used method for thresholding in CR is by fixing the threshold at an apriori known noise level [128, 129, 130, 131]. However, this approach often produces erroneous results whenever the noise samples begin to cross the threshold. One solution is to adapt the threshold to change according to the instantaneous state of the spectrum. This will lead to an Adaptive Threshold Technique (ATT) capable of keeping false alarm at a low rate. However, any practical ATT should have the capability to threshold without apriori knowledge of the noise level or Licensed User (LU) signal, and it should require little or no manual parameter adjustment within the algorithm. Finding or developing such an algorithm remains a tall order in the field of ATTs in CR. However, we have sought out such an algorithm, the Otsu algorithm in Image Processing [134], which fulfils all these characteristics. Otsu's algorithm selects a global threshold value by maximizing the separability of classes in the gray levels of an image. This technique has been modified for CR purpose by Onumanyi in [3]. However, to the best of our knowledge, this work has been the first place where this technique was used in a wavelet-edge detection method. Thus, we adapted the algorithm to work directly on the wavelet coefficients as follows:

In CR, the PSD of a given band can be easily sensed by the front-end of an ED. The sensed signal after scale decomposition using 3.3 can be represented in L grey levels $(1, 2, \ldots, L)$. The coefficients at levels i are denoted as fi; then, the total number of samples N will equal $N = f_1 + f_2 + \cdots + f_L$. Thus for a given spectrum dataset, the occurrence probability of gray levels i is given by

$$p_i = \frac{f_i}{N}, \quad p_i \geqslant 0, \quad \sum_{i=1}^{L} p_i = 1, \tag{3.13}$$

The aim is to divide the wavelet coefficients of the decomposed spectrum into two classes, C_1 and C_2, by a threshold at level t, where class C_1 consists of coefficients from 0 to t and class C_2 contains the other coefficients from $t+1$ to L. Therefore, the cumulative probabilities (w_1 and w_2) and mean levels (μ_1 and μ_2) for classes C_1 and C_2, respectively, are:

$$\omega_1 = \sum_{i=1}^{t} p_i, = \omega(t) \tag{3.14}$$

$$\omega_2 = \sum_{i=t+1}^{L} p_i, = 1 - \omega(t), \tag{3.15}$$

and

$$\mu_1 = \sum_{i=1}^{t} \frac{i \times p_i}{\omega_1} = \frac{\mu(t)}{\omega(t)}, \tag{3.16}$$

$$\mu_2 = \sum_{i=t+1}^{L} \frac{i \times p_i}{\omega_2} = \frac{\mu_T - \mu(t)}{1 - \omega(t)}, \tag{3.17}$$

where

$$\omega(t) = \sum_{i=1}^{t} p_i, \tag{3.18}$$

and

$$\mu(t) = \sum_{i=1}^{t} i \times p_i. \tag{3.19}$$

The total mean level of the data sample is

$$\mu_T = \mu(L) = \sum_{i=1}^{L} i \times p_i. \tag{3.20}$$

The class variances is obtained as

$$\sigma_1^2 = \sum_{i=1}^{t} (1-\mu_1)^2 \, pr(i|C_1) = \sum_{i=1}^{t} (1-\mu_1)^2 \, \frac{p_i}{\omega_1}, \tag{3.21}$$

$$\sigma_2^2 = \sum_{i=t+1}^{L} (1-\mu_2)^2 \, pr(i|C_2) = \sum_{i=t+1}^{L} (1-\mu_2)^2 \, \frac{p_i}{\omega_2}. \tag{3.22}$$

In adapting the Otsu's algorithm to the wavelet coefficients, the following discriminant criterion measure are stated and used in the discriminant analysis as

$$\lambda = \frac{\sigma_B^2}{\sigma_W^2}, \quad \kappa = \frac{\sigma_T^2}{\sigma_W^2}, \quad \eta = \frac{\sigma_B^2}{\sigma_T^2}, \tag{3.23}$$

where

$$\sigma_W^2 = \omega_1 \sigma_1^2 + \omega_2 \sigma_2^2, \tag{3.24}$$

$$\sigma_B^2 = \omega_1 (\mu_1 - \mu_T)^2 + \omega_2 (\mu_2 - \mu_T)^2 = \omega_1 \omega_2 (\mu_2 - \mu_1)^2, \tag{3.25}$$

$$\sigma_T^2 = \sum_{i=1}^{L} (i - \mu_T)^2 \, p_i, \tag{3.26}$$

given that

- σ_W^2 the within-class variance of the histogram of data samples,
- $\sigma_B^2$is the between-class variance of the data histogram, and
- σ_T^2 is the total variance of levels,

therefore

$$\sigma_T^2 = \sigma_W^2 + \sigma_B^2. \tag{3.27}$$

To obtain the desired threshold, an optimisation problem to search for a threshold t that maximises one of the objective functions in 3.23 is established. The discriminant

criteria that maximises η, λ, κ, for t are equivalent to one another. However, η is chosen because it is the simplest measure with respect to t. The optimum threshold t^* that maximises η is selected in a sequential search by using the simple cumulative quantities as

$$\eta(t) = \frac{\sigma(t)^2}{\sigma_T^2}, \tag{3.28}$$

$$\sigma_B^2(t) = \frac{[\mu_T \omega(t) - \mu(t)]^2}{\omega(t)\,[1 - \omega(t)]}. \tag{3.29}$$

and the algorithm is developed to select an optimal threshold t^* that maximizes the between-class variance σ_B^2 , based on the discriminant analysis given as

$$\sigma_B^2(t^*) = \max_{1 \le t \le L} \sigma_B^2(t) \quad w.r.t \quad 0 \le \omega(k) \le 1. \tag{3.30}$$

Thus, equation 3.30 becomes an optimisation search problem to find the optimum threshold that maximises the between-class variance. Essentially, the between-class variance is a measure of the separation in the probability distribution function, between the distribution of the noise and the signal samples within the dataset. Hence, it is expected that the optimum threshold will provide the widest separation between the noise and signal distribution within the signal. This is normally achieved by varying the threshold value, t, across the data histogram (which approximates the signal distribution) until the optimum threshold is obtained using 3.30.

3.4 Proposed Algorithm

3.4.1 Adaptive Wavelet-Based Space Scale Filter Algorithm

Algorithm 2 presents a summary of our proposed AWSSF.

Algorithm 2 Adaptive Wavelet-Based Scale Space Filter

1: Inputs: **wname: Haar**, the mother wavelet; **Level**, the required number of scale decomposition levels; **dataset**, the input data (PSD).
2: Compute the wavelet coefficients for different decomposition levels using equation 3.3
3: Correlate the different decomposition levels across the scales using equation 3.4.
4: Apply the Otsu multi-threshold algorithm to each correlated scale level to generate a threshold based on equation 3.30
5: Select the last correlated level and use its threshold (from step three) to classify the data.
6: Find peaks in the classified correlated data.
7: Use peaks to determine signal edges and boundaries
8: Use the edge location to generate a spatial filter (synonymous to a rectangular window of unit step).
9: Multiply the spatial filter by the original signal (dataset)
10: Obtain the detected PU signal

The contributions made in the AWSSF are:

1. The adaptation of Otsu's algorithm into the WSSF algorithm to introduce dynamism and adaptability.

2. The introduction of the concept of the peak finding algorithm to automatically identify the boundaries within the wavelet coefficients, which differentiates our AWSSF from the original WSSF.

3. The use of the last decomposition level of the coefficients for final detection rather than any other level as in [127, 128, 129]. This idea was motivated by the fact that the last level contains the lowest frequency components, which provides the clearest distinction between signal and noise.

3.4.2 Method of Simulation and Analysis

The algorithms were developed and evaluated in MATLAB version *13* on an Intel Core$^{\mathbf{TM}}i5$ processor at *2.53 GHz* and *4GB* RAM. It is noteworthy that the current

focus in SS in CR lies in the low SNR region, i.e., typically at about or below *0 dB*. Thus, the demonstration seeks to show the algorithm's capability only in the low SNR condition, rather than in the high SNR region, where performance is typically acceptable for all SS techniques. Hence, we simulated a Licensed User (LU) OFDM signal (with a *5MHz* bandwidth) in the time domain buried totally in noise at about *-10dB*. This was estimated using the ED, modelled using a Periodogram (with standard functions available in MATLAB). The output of the ED is shown in Fig. 3.1, wherein the LU signal is buried totally in noise (not visible above the noise level). The average noise power is set at *-20 dBm* with a standard deviation of about *20 dB*. The AWSSF's task is to detect this signal without knowledge of the noise level, or even the position of the LU signal. For analysis, we used the Receiver Operating Characteristics (ROC) curve. Details on how to develop ROC curves can be seen in [135]. Noteworthy is that at this point, Otsu's adaptive threshold was used here within the AWSSF, that is, on the wavelet coefficients, and not on the final real signal, which is what the ED typically operates on. Therefore, after computing the adaptive threshold and obtaining the filtered real signal from the final output of the AWSSF, the ROC curves was then used on the final real signal in the frequency domain (see Fig. 3.5) to compare with the ED.

3.5 Results and Discussion

The results presented here are based on the data in Fig. 3.1. The buried LU signals are located between the frequency indexes of 240 -315. Thus, the detector's job is to detect these samples located within this band without prior knowledge of their location (this is the expected scenario of operation for a typical CR).

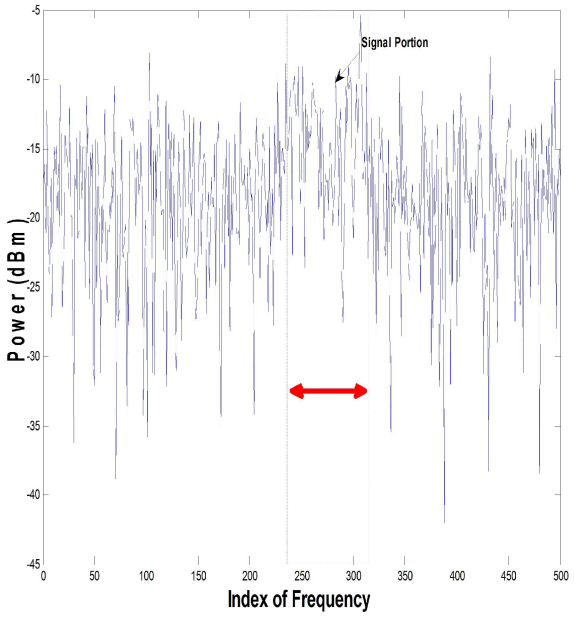

Figure 3.1: Low SNR Signal (*-10dB*)

3.5.1 In Low SNR Condition

Here, Fig. 3.2 provides the sample results of the estimated wavelet coefficients at levels 1, 2, 5 and 6. Other levels are omitted (that is, 3 and 4) because they were not used in the processing, and they do not add any value to the discussion (see Algorithm 2). The dotted red boxes in the result of Fig. 3.2 denote the portions belonging to the LU signals embedded in noise. Observe that the coefficients are typically similar to noise at lower levels (1 and 2), see Figs. 3.2a and 3.2b, while the coefficients get slower at higher levels (5 and 6) as shown in Figs. 3.2c and 3.2d. In this work, a maximum of six levels was used, because, above this value, nothing much can be deduced of the signal characteristics (since only the slowest samples of the signal are available and they become unusable after this level). Observe that by using the wavelet coefficients alone in Fig. 3.2, it is practically impossible to achieve detection using threshold. Hence, the proposed AWSSF was used to directly multiply adjacent scale levels. In

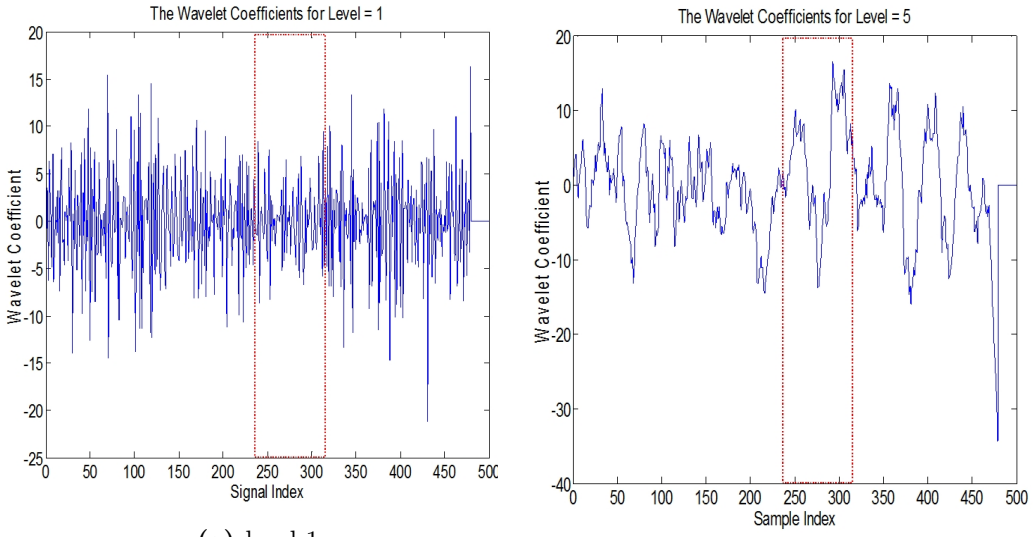

(a) level 1

(c) level 5

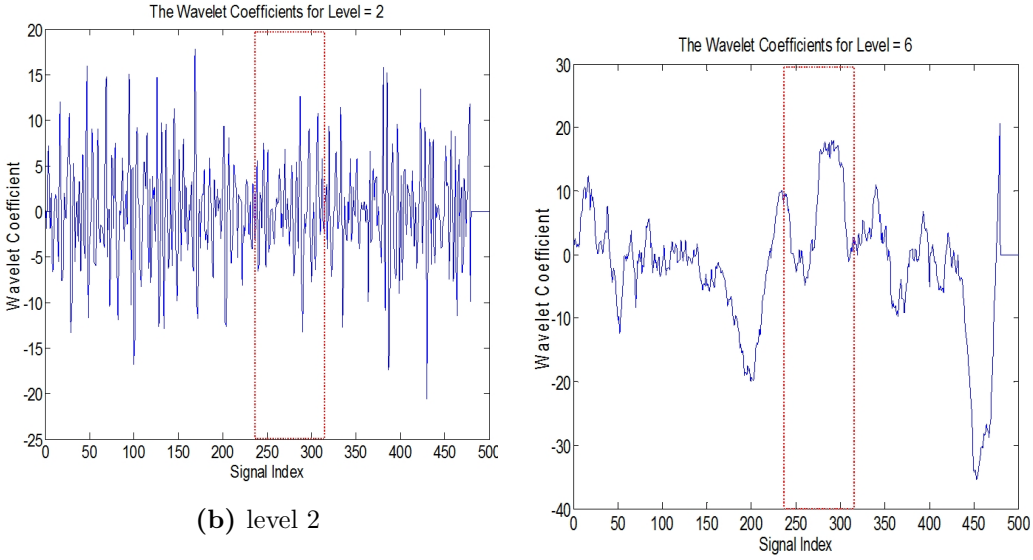

(b) level 2

(d) level 6

Figure 3.2: Wavelet Coefficients estimated for -10 dB signal.

this case, for a total of 6 levels, multiplication of adjacent levels provided us with 5 sample levels. However, only results of the correlations between levels 1 and 2, Fig. 3.3a and levels 5 and 6, Fig. 3.3b were presented.

Fig. 3.3 shows the absolute values of the multiplied coefficients between levels *1* and *2* and levels *5* and *6*. Observe that the multiplication between levels *1* and *2*

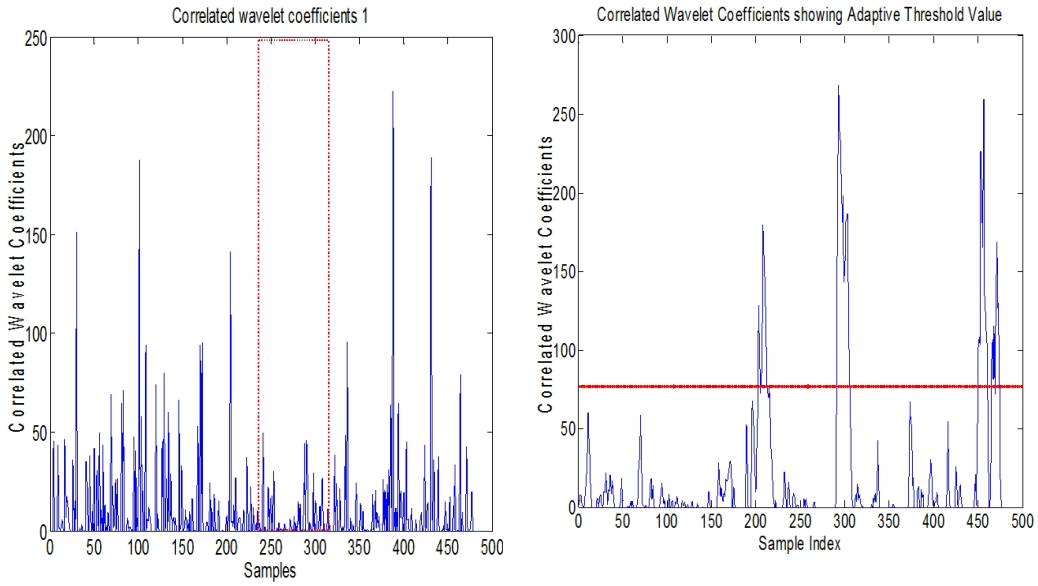

(a) CWC between levels 1& 2

(b) CWC between levels 5& 6

Figure 3.3: Correlated Wavelet Coefficient (CWC) between scale Levels 1 and 2, and between Levels 5 and 6.

contains several high rising peaks (see Fig. 3.3a), which makes it difficult to detect the signal (within the red box) without incurring a high false alarm rate. However, at higher multiplication levels (between 5 and 6) (see Fig. 3.3b), it can be observed that the noise level greatly diminish thereby, allowing the signal boundaries to be more pronounced. Based on our concept of adapting Otsu's algorithm (in AWSSF), an adaptive threshold was estimated at value *75* (see Fig. 3.3b), which was then used to classify signal edges from noise in Fig. 3.4 (according to Algorithm 2).

Next, Fig. 3.4 shows the samples residing above the threshold (after Otsu's algorithm), which will be used for detection. Note that the falling edges (red line in Fig. 3.4) were used by the AWSSF to compute the actual location points of the signal boundaries (using the peak finding algorithm). However, due to the low SNR region being considered (at -10 dB), the algorithm still misclassified some spurious false samples as seen at the 450th sample (see Fig. 3.4 within the blue box). This

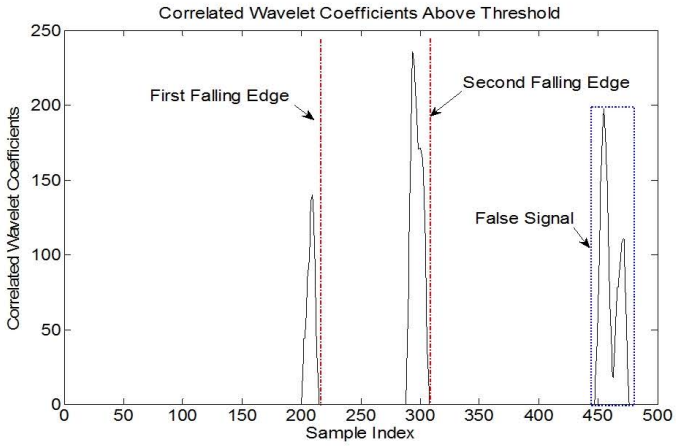

Figure 3.4: CWC detected above the threshold (estimated by Otsu Algorithm).

is typically inevitable at such a low SNR level. However, owing to the detection mechanism used in the AWSSF (within the peak finding algorithm), the AWSSF algorithm requires two peaks to be identified continuously when counting from left to right to form a bounded region belonging to an LU signal. Thus, in a case whereby only one peak exists (see false signal portion in Fig. 3.4), the algorithm discards such points, thereby eliminating the false signal. As a result, the AWSSF kept only the boundaries shown by the dotted red lines in Fig. 3.4, because it had a bounded edge (two edges). The algorithm used these boundaries to create a spatial filter in Fig. 3.5a, which was then multiplied directly with the original signal (of Fig. 3.1) to arrive at the final detected signal (embedded within noise) as shown in Fig. 3.5b. It can be clearly seen (in Fig. 3.5b) that the signal portion was detected by the AWSSF algorithm without prior knowledge of its location.

3.5.2 Comparison with Energy Detector(ROC Performance)

AWSSF was compared with the Energy Detector (ED) at the same low SNR level (using data of Fig. 3.1 for both detectors). This was to show the level of performance achievable by the AWSSF. It can be seen from the results in Fig. 3.6 that the AWSSF

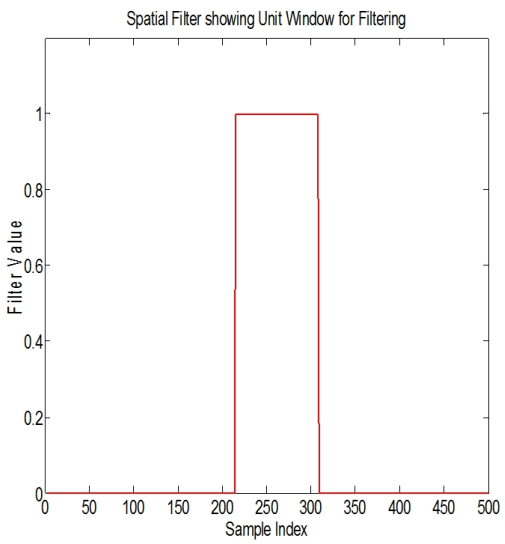

(a) Spatial filter

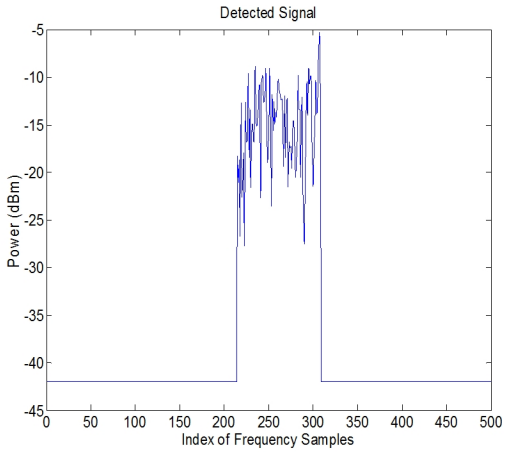

(b) Final detected signal

Figure 3.5: Spatial Filter for detecting signal and the Detected Signal

provided a better ROC performance than the ED. Notice that the ED's ROC is only at about 40 % detection rate at a false alarm rate of 10%. Thus, the AWSSF can be considered an effective alternative to the ED in low SNR detection conditions in CR because it achieved a remarkable 90 % detection rate at 10% false alarm rate.

3.5.3 Discussion on related approaches

For the purpose of analysis, we used an OFDM signal occupying a 5 MHz bandwidth and totally buried in noise to evaluate the low SNR region. This test at *-10dB* is lower than Tian *et al.*, [128], who though used a wider band spectrum, had their lowest signal at about *4dB* (see [[128], pp.4]). Their approach had a relatively low complexity of $O(N)$. We note that the extent of bandwidth may not be the focus here but rather the detection and false alarm performance of these techniques. Wang *et al.*,[127] on the other hand provided results as low as -25 dB, however, this required a threshold influence ratio to be optimised, which will be unrealistic in the real-time

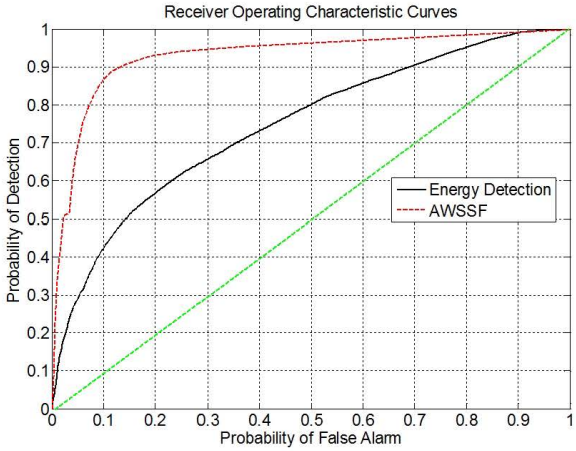

Figure 3.6: ROC Curves at Low SNR (-10dB).

operation of their algorithm. Thus, we analysed and discussed the performance of these techniques at the *-10dB* level. The result of our comparison is provided in Table 3.1. It can be seen in [127] that Tian *et al.*, did not provide quantitative performance analysis in their work. However, they provided graphical results of the wavelet coefficient outputs in their paper showing how their signal detection was visualised. In addition, apart from not using adaptive thresholds, their region of interest can be classified as high SNR region, compared to the other approaches in Table 3.1. The AWSSF also performed better than Wang *et al.*,[127] in the false alarm rate, and better than Zhao *et al.*,[131] in the detection rate. Summarily, while others did not meet the IEEE 802.22 standard requirement of 90% detection and 10 % false alarm rate, it should be noted that the AWSSF met these requirements (see Fig. 3.6) with a complexity of $O(N)$ in addition to its adaptivity. This makes our approach viable for effective application in CR.

Table 3.1: Comparison of related spectrum sensing techniques (N is total number of samples)

Technique	**Complexity**	**SNR (dB)**	**Detection (%)**	**False Alarm (%)**
Wavelet-Based Wideband technique[128]	$O(N)$	4	-	-
Adaptive Based ED [127]	$O(N)$	-10	100	50
Subspace SS [136]	$O(N^3)$	0	90	0.03
Zhao *et al.* [131]	$O(N)$	-10	60	10
AWSSF	$O(N)$[137, 138]	-10	90	10

3.6 Chapter Summary

This Chapter has presented the Adaptive Wavelet-based Scale Space Filter (AWSSF) algorithm for spectrum sensing in Cognitive Radio. The results obtained showed that the algorithm achieved a 90% detection rate at 10% false alarm rate, as compared to the 40% detection rate at same false alarm rate for the Energy Detector (ED). It was also shown that the AWSSF performed better than other Adaptive Wavelet based techniques seen in the literature. Though AWSSF is more complex than the traditional ED, due to the number of sample multiplications required, it however provides higher accuracy, which is quite essential for CR operation. Thus, while the current state of the AWSSF algorithm can be considered viable for CR deployment, future works will focus on reducing complexities and achieving better performance in the low SNR region.

Chapter 4

Dynamic Control Channel Protocol for Cognitive Radio Ad-Hoc Network: Ant Colony System Implementation*

4.1 Introduction

Dynamic Spectrum Access (DSA) is a critical function of Cognitive Radio and has formed an area of recent research interest. This interest ranges from developing robust, broad band sensing techniques to co-tier and cross-tier interference issues among Secondary Users (SUs) and Primary Users (PUs or licensed users), in addition to improving Quality of Service (QoS) with respect to channel access. With the aim of improving channel access, this chapter presents the proposed adaptation of the

*The contents of this chapter are from Ohize and Dlodlo [139]

ACO in the selection of the 'stay' channel. The 'stay' channel selection is for the purpose of constructing a channel hopping algorithm as presented in Chapter 5.

With respect to known solutions, fixed or preselected common control channel (CCC) techniques for MAC protocol design have been proposed to address these challenges. However, this has opened up more challenges such as control channel security, robustness to PU activities, control channel coverage and control channel saturation[88]. Recently, the most patronised solution is the use of dynamic CCC (DCCC) for CRAHN [24, 92]. DCCC facilitates a variety of operations from a transmitter-receiver handshake, neighbour discovery, channel access negotiation, topology change and routing information updates, to cooperation among CR users [24, 140]. It was noted that DCCC in some texts is typically linked to the concept of channel hopping CH [92]. But in this chapter, the use of ACS as a channel ranking algorithm to rank channel sets detected by an SU is proposed. This ACS approach combined with the hopping sequence developed in [126] forms a selection scheme for the selection of control channel, which will be presented in Chapter 5.

The use of ACS methods for coordination and organisation of network routing parameters have been observed in the literature, an example is the AntNET. Also in [141] Dorigo and Gambardella employed ACS in solving the travel salesman problem. By drawing similarities, this technique was adopted for achieving the goal of coordination among CRAHN nodes. In this chapter, CRAHN nodes were deployed randomly amidst PU presence in an overlay spectrum sharing mode. SUs detect spectrum holes, transmit on these spectrum holes and prepare a list of ranked spectrum hole information array (SHIA) towards the selection of a 'stay-channel' for the hopping sequence (HS) in chapter 5. SHIA is then employed in the HS to guide nodes toward rendezvous on a CC. The concept of ACS was adopted, as pheromone trails are deposited on channels of quality paths.

Some related works have been shown in literature in respect of DCCC design scheme. Some notable CCC designs can be found in [24]. However, on techniques which implement a DCCC selection scheme, and an ACS scheme, we take a look at some closely related designs. In [94] Chen *et al* addressed control channel assignment problem by employing the use of Hello beacon messages as pheromone trait to rank channels, this expedites the control channel selection process. In their work, the channel ranking was based on a Q non-negative real value, inversely proportional to the interference imposed by the surrounding PUs. However, in our work the channel ranking is based on a combination of; channel availability $l_{m,n}$, commonality of channel $c_{m,n,k}$ and received signal strength (RSS) $\gamma_{m,n,k}$ on a given channel. These factors form our cost function or objective function as seen in equation 4.4.

Also in [142] He and Zhang employed the ACO technique for dynamic channel assignment. Their unique application of the ACO addressed optimal channel assignment for the various CR nodes. They did not formulate the control channel selection problem in their work. Similarly, in [143] the authors applied the ACS for spectrum allocation in CRAHN, again in both cases the control channel selection problem was not addressed. Despite various unique contributions, some gaps were noted in the existing works. To address the problems, an ACS approach for channel ranking towards developing an adaptive control channel scheme was proposed.

The objective of this chapter is to propose and demonstrate a step by step adaptation of the ACO towards the selection of the 'stay' channel. The rest of this chapter is organised as follows; Section 4.3 describes the network model, Section 4.4 explains the general system algorithm, Section 4.5 describes the simulation setup,the results and discussion while the summary is presented in Section 4.6.

4.2 Justification for the use of ACO

In EAs, each algorithm's performance is largely affected by their specific parameters. The choice of values associated with these specific parameters may improve or reduce EAs performance regarding of the solution quality and the processing time[104]. For example, in GAs, the main parameters affecting its performance are the population size, the number of generations, crossover rate, mutation rate and the complexity of the objective function[144]. Larger population size and a large number of generations increase the likelihood of obtaining a global optimum solution but substantially increase processing time[104]. For the MAs, same parameters are employed similar to the GAs, but they apply local search on chromosomes and offsprings. In the case of ACOs, the parameters of interest are the number of ants, the number of iteration, the pheromone evaporation rate, the objective function and the application dependent constant β and α. Whereas the PSO specific parameters include; the numbers of particles, generations, the maximum velocity, the inertia weight factor and for the SFLA, the parameters are, the population of frogs, the number of memeplexes, and he number of iterations. A comparative study of five EAs discussed in Chapter 2 based on the problem identified in literature is presented in this section. Results presented to justify the choice of the ACO technique.

In [104] the authors applied the the GA, ACO, PSO, MA and the SFLA to solve the discrete time-cost trade-off (TCT) construction management problem. The problem relates to an 18- activity construction project, detailed in [145]. To obtain the most suitable parameter values that suit the test problems, a large number of experiments were conducted. For each algorithm, an initial setting of the parameters was established using values previously reported in [146, 118, 147, 119, 148]. After that, the parameter values were changed one after the other and the results were

monitored regarding the solution quality and speed. Table 4.1 presents the results obtained in [104] indicating the ACO as the fastest regarding the processing time.

Table 4.1: Comparison of the EA techniques

Algorithm	**Minimum project duration (days)**	**Average cost ($)**	**Processing time (s)**
ACOs	110	166,675	10
MAs	110	162,495	21
GAs	113	164,772	16
PSO	110	161,940	15
SFLA	112	166,045	15

4.3 General System Model

4.3.1 Network Description

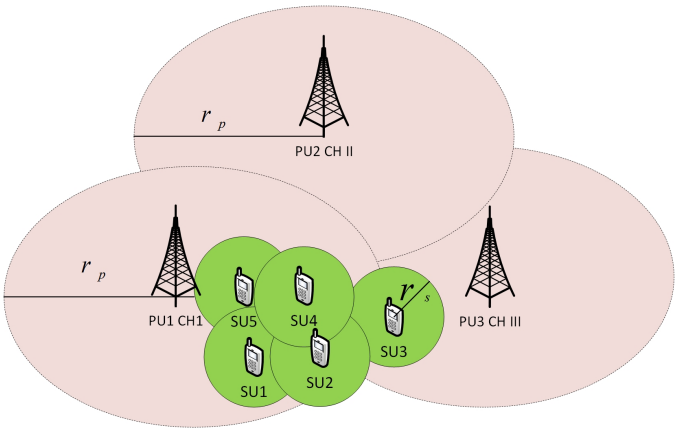

Figure 4.1: Network Topology with PUs 1, 2 & 3 on channel I, II & III respectively

In this section, a two-tier network is described as shown in Fig. 4.1 which comprises of J primary base stations and N secondary users, where $J = 3$ and $N = 5$. SUs are

equipped with OFDM technology and randomly deployed within the network. We use OFDM to utilise M multiple channels for the purpose of providing connections for devices within the CRAHN. The M channels are uniquely indexed from 1 to 5. Each PU j occupies one of the M channels and transmits within a circular area of radius $r_p(j,m)$. The overlay spectrum sharing mode does not allow SUs within radius $r_p(j,m)$ to use channel m taken up by PU j. Similarly, n SUs with a fixed coverage radius of $r_s(n,m)$ on one of the channels m is deployed randomly as shown in Fig. 4.1. Interference mitigation is achieved through conflict-free spectrum allocation as shown in Fig. **??** and defined in section 4.3.2. In a real sense, fast and accurate spectrum sensing is needed to enable conflict-free spectrum allocation, and this remains an open research issue in CR. However, in Chapter 3 an AWSSF algorithm was proposed to further enhance sensing accuracy. Since an SU can only detect PU's activity within the PU's transmission range, we apply a binary geometry model where an SU conflicts with the PU if they are located within a certain distance from each other.

4.3.2 Channel Model

Measurements have shown that at any distance d, the path loss $PL(d)$ at a particular distance is random and distributed log-normally about the mean distance-dependent value [149]. Therefore the RSS $y_{m,n,k}$ at node k receiving a beacon message from its neighbouring SU nodes n, on channel m is modelled with the log-normal shadowing path loss model as shown in equation 4.1 below,

$$y_{m,n,k} = A - 10n_p \log_{10}(D_{n,k}) + \varphi_m, \tag{4.1}$$

where φ_m is a zero-mean Gaussian distribution. It accounts for the random shadowing effect which occurs over a large number of measurement location even with same Tx-Rx separation. A is the received signal strength (RSS) at one-meter reference distance, and n_p is the propagation path loss exponent. $D_{n,k}$ is the distance between nodes n and k.

SU Channel availability L

SU n, Channel availability $l_{m,n}$ is an M by N matrix defined as $L = \{l_{m,n} | l_{m,n} \in \{0, 1\}\}$, where

$$l_{m,n} = \begin{cases} 1 & r_s(n,m) \leq D_{n,j} - r_p(j,m) \\ 0 & otherwise. \end{cases}$$

Fig. **??** depicts this expression. Where $D_{n,j}$ is the distance between SU node n and PU j and $l_{m,n}$ defines the availability of channel m for SU node n.

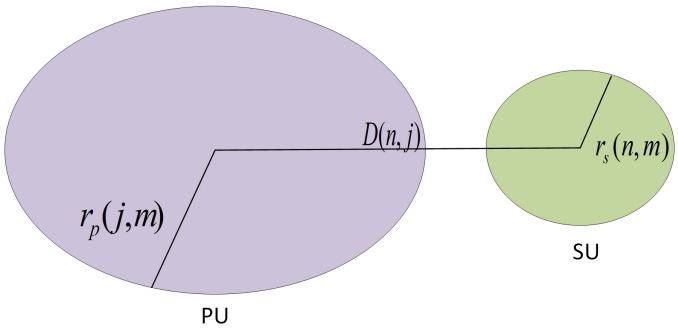

Figure 4.2: Free spectrum assignment on channel m($l_{m,n} = 1$)

Common channel C

For two radios to communicate on a CRAHN, AT least a common channel must exist between the radios. We define a common channel matrix that defines the channel

availability for the two communicating radios n and k as $C = \{c_{m,n,k} | c_{m,n,k} \in \{0,1\}\}$ where

$$c_{m,n,k} = \begin{cases} 1 & l_{m,n} * l_{m,k} = 1 \\ 0 & otherwise. \end{cases}$$

User reward metrics

A user reward metrics is a reward vector for user n on channel m communicating with node k defined as

$$R_{m,n,k} = a_{n,k} \times c_{m,n,k} \times b_{m,n,k} \tag{4.2}$$

where $a_{n,k}$ is a range vector defined as

$$a_{n,k} = \begin{cases} 1 & d_{n,k} \leq d_{th} \\ 0 & otherwise. \end{cases}$$

Here $a_{n,k}$ only ensures that the two communicating radios n and k on channel m are within each other's transmission range threshold d_{th}. And

$$b_{m,n,k} = B_0 \times log_2(1 + \alpha \times \gamma_{m,n,k}) \tag{4.3}$$

$b_{m,n,k}$ is the utility or capacity on channel m enjoyed by SU n receiving a beacon message from one of its neighbouring node k assuming there is no interference. Note that α is a constant signal-to-interference-plus-noise ratio (SINR) gap of AWGN channel to meet the target bit error rate (BER)and is defined as $\alpha = -1.5/ln(5BER)$. For simplicity, the channels are considered to be m non-overlapping orthogonal channels so that each channel has a bandwidth of $B_0 = B/M$. B is the entire network bandwidth.

4.3.3 ACS Model

Ant colony system is a class of algorithms that have been used for the organisation and optimisation of network parameters, and it was first proposed by Dorigo [141]. The ACS imitates the behaviour of real ants in constructing optimal routes from food source to their nest and vice versa, using exploration and exploitation search methods that involve depositing pheromone trails on the channel, proportionate to the cost function derived. The main novel idea is the synergistic use of cooperation among many relatively simple agents which communicate through the distributive memory implemented as pheromone deposited on edges of a graph.

Path-finding on a graph:ACS

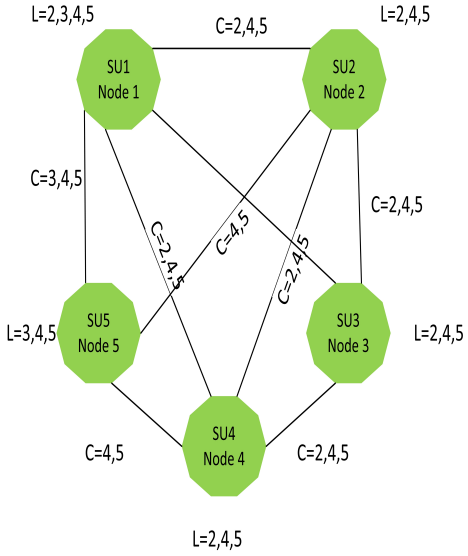

Figure 4.3: Graph of Network Fig. 1

In the proposed algorithm, artificial ants move between discrete states in discrete paths. Since the network is discrete in nature, it may be represented by nodes N and route M, where N and M correspond to the SUs and channels, respectively. The complex objective of selecting optimal control channel is reduced to a graph. The

network model is extended to representing control channel assignment. Therefore a bi-directional graph G = (N,L,C) is defined, where N represents the set of SU nodes that share the available spectrum L, and C is the arc or edge that represents sets of common channels between two nodes. Fig. 4.3 is the graph solution of Fig. 4.1 $L\&C \in M$ were defined in subsections 4.3.2. The problem is how to find a set of arc flow that maximises link reward.

Objective function for Optimal Control channel selection

The control channel selection scheme returns a channel m that maximise network reward between node n and k and assign it as a candidate solution for our stay channel in the CHS described in Chapter 5. The objective function which is also the cost function is shown in equation 4.4

$$R(m) = \sum_{n=1}^{N} \sum_{k=1}^{K} a_{n,k} * c_{m,n,k} * b_{m,n,k}, \tag{4.4}$$

subject to $a_{n,k} \leq 1$ [Ensures nodes are within transmission range],

and $c_{m,n,k} \leq 1$ [Ensures atleast a common channel exist].

The ACO returns as solution the best channel as shown in equation 4.5

$$A = arg \max R(m) \tag{4.5}$$

Computing Pheromone Update

In ACO, pheromone secreted along the selected path is based on the equation 4.6 which shows a direct relationship between the deposited pheromone and the cost function.Therefore, higher rewarding channels will have higher pheromone deposit.

$$\tau_{m,n,k}(t) = \tau_{m,n,k}(t-1) + QR(m)^z, \tag{4.6}$$

again $\tau_{m,n,k}$ is the deposited pheromone, z is the selected ant whose returned value is the optimal and Q is a constant. For pheromone evaporation, the equation is

$$\tau_{m,n,k} = (1-\rho)\tau_{m,n,k}, \tag{4.7}$$

ρ is the pheromone evaporation coefficient which gives the relative contribution of the previous solution to the next solution. Subsequent ants are most likely going to select the path with the most pheromone along its trail with probability as shown in equation 4.8.

$$pr^z_{m,n,k}(t) = \frac{\tau_{m,n,k}}{\sum_{k=1}^{P} \tau_{m,n,k}}, \tag{4.8}$$

where: $pr^z_{m,n,k}$ is the probability of the z^{th} ant to move from node n to node k on channel m at the t^{th} iteration/time step. P is the total number of ants.

A colony of ants (z) is generated to find possible solutions subject to the condition of highest reward along a selected path. The decision at each node on which path to select next is made using a Roulette Wheel Selection algorithm as seen in [150].

4.4 General System Algorithm

4.5 Simulation set-up, results and discussions

The evaluation of the performance of the designed two-tier network is done using MATLAB. The network parameters are in accordance with the IEEE 802.22 standards [38]. Table 4.2 shows the simulation parameters of the designed two-tier network.

Algorithm 3 Ant Colony Optimisation Algorithm

```
1: procedure BEGIN
2:     while termination condition is not met do
3:         for ant z=1 to 'P total number of ant ' do
4:             Move ant(z) between pairs of nodes (n,k)
5:             Use Roulette Wheel Selection Algorithm to choose common channel
   between nodes.
6:         Compute the cost of using the channel choice for the network using
   equation 4.4.
7:         Compare cost with the best route
8:         if cost is higher then overwrite best route with new channel choice,
9:         else Maintain best channel choice
10:        Update pheromone trail using equation 4.6
11:        Perform evaporation
```

The propagation environment model is that of a shadowed urban cellular radio environment with obstructing buildings. In the network, we deployed j PUs in fixed location while the SUs were deployed randomly as described in section 4.3 Fig 4.1. This experiment was performed over 1000 iterations with 50 ants deployed across the SU nodes. The ACS parameters used are $\rho = 0.1$, $\alpha = 0.3$. These ants forage across the network (graph) in search of the optimal channel for control channel selection. The detailed MATLAB implementation is shown in Appendix B.

The developed algorithm was implemented and ran on MATLAB with 10 SU nodes being considered. The transmitting and receiving nodes were observed. Nodes that are within transmission range and have common set of channels were selected. The algorithm was tasked with finding a channel with the most reward between these communicating nodes. The result as observed is shown in Table 4.3. This simply validated the efficacy of the ACO has a feasible solution for 'stay' channel selection. In Table 4.3 node 10 communicates with node 8 and the best channel returned is 9 with an associate cost of 2328.2483. In summary, the returned value is used as the 'stay' channel in the CH algorithm of Chapter 5. The details of the CH algorithm will be shown in the next chapter.

Table 4.2: Network Simulation Parameters

Parameters	Value (Unit)
Network Model	Two tier, Urban network, 250m radius WAN
PU Coverage radius	100 m
SU Coverage radius	35 m
Path loss exponent n_p	4 (urban network)
Variance for log-normal shadowing	8 dB
Path loss constant A measured for 1 m	6 dB
Channel Bandwidth	6 MHz
Number of Channels M	10
Number of PU J	3
Number of SU N	10
BER	5

4.6 Chapter Summary

This chapter has provided a step by step demonstration of the proposed control channel selection scheme using the ACS approach. This chapter formulated the selection of a control channel as a path searching problem in a graph and used pheromone trail to guide the construction of an optimal solution. A cost function that evaluate each channel based on RSS, channel availability and common channel among other network nodes was developed. Chapter 5 presents the application of the ACS in a channel hopping algorithm towards the selection of the control channel.

Table 4.3: Network Simulation Result

Source Node	Receiving node	ACO Channel returned	Optimal Cost
10	8	9	2328.2483
5	6	10	2452.2877
8	7	7	2321.9812
8	9	8	2261.9132
8	6	8	2388.4712
5	7	9	2511.2312
10	7	9	2521.3411
9	7	9	2372.2827
6	10	10	2426.3838

Chapter 5

Ant Colony System Based Control Channel Selection Scheme for Guaranteed Rendezvous in Cognitive Radio Ad-hoc Network*

5.1 Introduction

Several spectrum surveys conducted across the globe revealed spectrum under-utilisation as opposed to scarcity. The major cause of this pseudo scarcity of spectrum is the current paradigm of allocation technique known as the "Command and Control Technique (CCT)". CCT is exposed to limitation, as every radio technology must have a predefined and distinct spectrum for communication. CCT has failed to identify underutilised bands. The trending solution is the use of unlicensed devices by secondary users (SU) in these underutilised bands opportunistically. The Federal

*The contents of this chapter are from Ohize and Dlodlo [126]

Communication Commission (FCC) in the United States of America, recently adopted this solution. The enabling technology for opportunistic spectrum usage is the Cognitive Radio (CR) technology.

CR is defined as a radio which is capable of identifying its spectral environment and able to optimally adjust its transmission parameters to achieve an interference-free communication channel. In CR technology, Dynamic Spectrum Access (DSA) is made feasible. However, spectrum access by the opportunistic user (SU) in CR must avoid co-tier and cross-tier interference, accurately detect spectrum and make decisions, and guarantee Quality of Service.

Most protocol design schemes have been proposed to suit multichannel CR network for centralised architectures such as IEEE 802.22 and Dynamic Spectrum Access Protocol. However, few have been designed for distributed networks which are also known as Ad-Hoc Networks. Ad-Hoc networks have zero form factor due to the absence of a central coordinator such as an access point or a base station. This has added to the complexity of developing a suitable MAC for CRAHN in addition to CRs spectrum heterogeneity, spatial and time-varying spectrum availability[91]. The introduction of fixed or preselected common control channel (CCC) in MAC protocol design has remained the favourite solution in most works. However, this technique leaves more to be desired. The fixed CCC is exposed to control channel jamming, coverage limitations and it is not always robust to PU activities. To this day the most favoured solution is the implementation of a dynamic CCC (DCCC) for CRAHN [24] [88]. DCCC facilitates a variety of operations from a transmitter-receiver handshake, neighbour discovery, channel access negotiation, topology change and routing information updates, to the cooperation among CR users. DCCC in some texts is implemented as a channel hopping technique[24, 140].

In this chapter, a swarm aided stay-jumping (SASJ) channel hopping algorithm for control channel selection scheme is developed. The channel hopping algorithm is constructed, such that, it reinforces channels with better characteristics in the solution pool, for selection as the control channel. This is done by returning a stay channel from the optimisation algorithm in chapter 4. It is shown that by employing the proposed algorithm we have improved on time to rendezvous on a common control channel. By rendezvous, reference is made to the process of convergence which occurs when each SU node seeking to communicate with another must first converge on a common channel to establish a link.

The concept of node convergence on a common channel in CR networks has gained tremendous attention in recent years. Channel hopping (CH) is one such technique where communicating CR nodes hop across different available bands. Horine & Turgut in [151] developed an algorithm for initial network connection, whereby nodes seeking to join the network randomly visit potential channels while emitting attention signals (side tone) of length equivalent to a single Fast Fourier Transform (FFT) frame. They demonstrated that a short duration narrow bandwidth with low power attention signal could be detected in a noisy environment. However, it was noted from their analysis that the process of rendezvous is not bounded in time and consist of several points of failure. DaSilva and Guerreiro in [90] used the predefined non-orthogonal sequence to determine the order for visiting potential channels in the process of achieving rendezvous. The predefined sequence involved a random permutation of N available channels, though no preference for rendezvous on the best channel was obtained for its time to rendezvous (TTR). Theis et al. [92] applied prime number modulo operation in addressing the blind rendezvous problem. They developed Modular Clock Algorithm (MCA) and a Modified MCA to address the weakness of MCA. MCA and MMCA showed considerable speed up in TTR. However, rendezvous was not bounded in time for all scenarios. In [152], Hai Liu *et. al.*

developed a robust Jump-Stay (JS) rendezvous algorithm that generates CH sequence in rounds for different CR nodes such that each round consists of two jump patterns; which is a random permutation of the M available channel and a stay pattern on any channel. They showed some improvements in TTR. Similar techniques (Enhanced Jump-Stay, EJS) were observed in [153],[154] and [155] with some modifications and improvements over [152]. In [156], CR nodes are made to hop on available channels with varying velocity such that rendezvous can be achieved by different CRs whereas in [157], CH schemes were generated in clockwise and counterclockwise orientation to achieve rendezvous. Another approach in solving the rendezvous problem is the use of quorum-based systems as shown in [93],[158], [159] and [160]. In these works, cyclic quorum systems were designed based on difference set theory. Despite varying unique contributions, some gaps were noted in the existing design, and we take further steps in addressing these. Existing designs do not consider the dynamic nature of CRAHN regarding the channel availability. This is factored into this work by computing the channel cost or reward based on channel availability as described in 4. Therefore, a Channel Hopping (CH) sequence based on the ranking system is constructed.

The rest of the Chapter is organised as follows; Section 5.2 describes our system design, Section 5.3 presents the general system algorithm, Section 5.4 looks at the system theorems, Section 5.5 covers the theoretical analysis while Section 5.6 describes the simulation set-up, results, as well as the discussions and conclusions are made in Section 5.7.

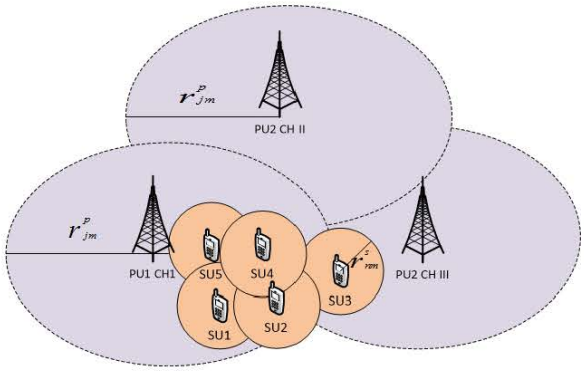

Figure 5.1: Network Topology with PUs 1,2 & 3 on channel I, II & III, respectively.

5.2 System Design

5.2.1 Basic System Model Description

The entire spectrum bandwidth is mapped into finite band spaces using a linear function. Here we consider the finite bands to consist of M non-overlapping orthogonal licensed channels. The PUs J are considered to be holders of M channels and are uniquely indexed $0, 1, 2, \ldots, M$. The two-tier network consists of SU nodes N such that $N \geq 2$ SU nodes share the channel with the PUs in an overlay architecture using OFDMA technology. Fig.5.1 describes the two-tier network. Each PU J occupies one of M channels and transmits within a circular area of radius r^p_{jm}. Similarly, the SUs node N opportunistically utilise m available channels not utilised by the PUs and transmit within a protective coverage area of a radius r^s_{nm}.

5.2.2 Problem Formulation

$G_{i,k}$ is defined as a set of available channels observed by SU nodes n and k such that $i, k \in N$ and $G_{i,k} \in M$. System rendezvous is feasible provided that at least a common channel exist, that is, $\cap G_{i,k} \neq \emptyset$. Time to Rendezvous (TTR) and Expected TTR (ETTR) are the two important metrics used to evaluate system performance.

This chapter assumes a time slotted transmission with a fixed transmission time slot. We define notation T as the minimum time taken to exchange control information between SUs. IEEE defines T as 10ms [161]. The scenario is asynchronous, so to ensure that complete beacon exchange occurs for overlapping hopping sequence the period of exchange is set to $2T$. For simplicity and comparative analysis, $2T$ is taken as equal to a unit time.

5.3 General System Algorithm

The general system algorithm is presented in the flow chart of Fig. 5.2.

5.3.1 Spectrum Sensing or Hole Information Array Technique

In a real sense, fast and accurate spectrum sensing is needed to enable a conflict free spectrum allocation, and this remains an open research issue in CR. Since an SU can only detect PU's activity within the PU's transmission range, we apply a binary geometry model where an SU n on channel m conflicts with the PU j if they are located within a certain distance r^p_{jm} from each other. Fig. **??** and section 4.3.2 describes how each SU node adopt the interference free spectrum model to prepare the hole information array (HIA).

5.3.2 Channel Ranking System using ACS

In this subsection, we make reference to section 4.4 where user reward metrics for ranking channels was introduced.

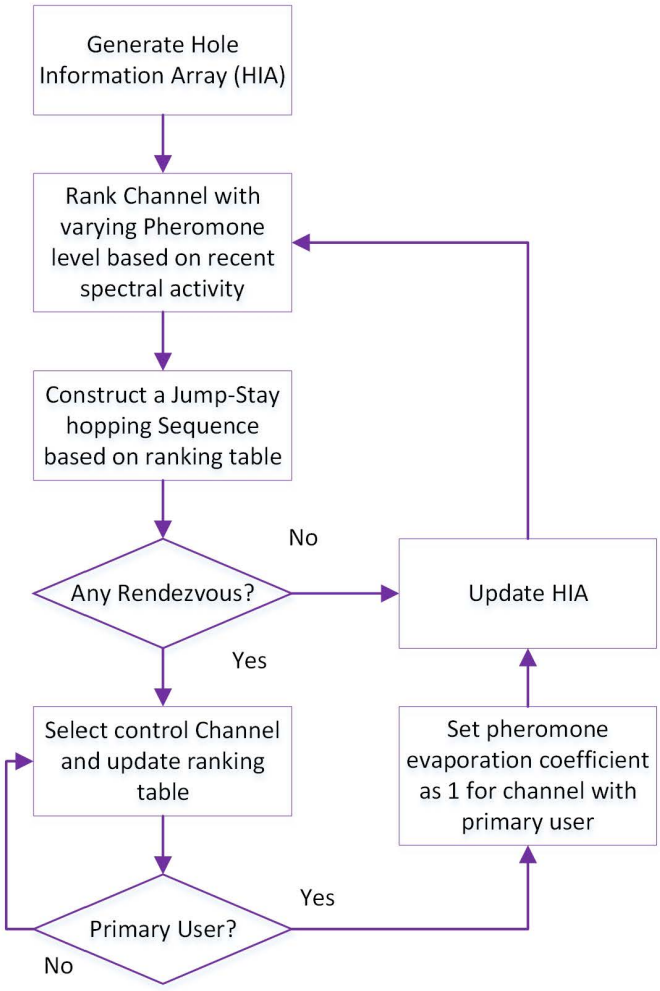

Figure 5.2: General System Algorithm

5.3.3 Constructing Stay-Jump Hopping Sequence

A new channel hopping CH sequence(CHS), the Swarm Aided Stay-Jump (SASJ) CHS is developed. This presents an original concept on how white spaces between PU transmissions should be visited by SU nodes to achieve rendezvous on a common coordination channel. The concept is to develop Stay-Jump CHS such that the most ranked channel is assigned the stay channel in the CHS. In this model each full cycle of hopping consist of; a stay-pattern on the most prominent channel (highest ranked channel) and two rounds of jump-pattern, a total of $3M_n$ time slots.

Stay Channel Selection for CH sequence

ACS technique is used to determine the channel m which maximises network reward between node n and k and which can be assigned as a candidate solution for selection as stay channel in the blind rendezvous problem.

Jump CH sequence

To further describe our CHS we define three key integers; M_n, is the number of available channel for radio n, r is the step length, usually an integer in [1, M_n]. For simplicity's sake let $r = 1$, since channels will be visited sequentially on the ranked table, i is the starting index, and it lies in the set [0, $(M_n - 1)$] which is usually the stay channel. The jump pattern J_p, last $2M_n$ time slots and the stay pattern S, last M_n time slot. In the stay pattern, the CR stays on the most ranked channel index i. Whereas in the jump pattern the SU starts on channel index i and keeps hopping in [0, $(M_n - 1)$] with step length r while performing the modulo operation around M_n. Similar works in literature utilised prime number P modulo arithmetic [152] to guarantee TTR under different rendezvous model. However, since P is the lowest prime number greater than or equal to M_n, there will always be gaps between M_n and P thus resulting in increased TTR [90]. Here we simply adopt a rap around M_n modulo arithmetic provided it is shown in Theorem one that the set of indexes R generated by the operation X mod M_n is a member set of [0, $M_n - 1$], where X is any positive integer. i.e $R = XmodM_n \in (0, M_n - 1)$

5.4 System Theorems

Theorem 5.1. *Given any number sequence X, such that $X, n \in \mathbb{Z}$, then the set of numbers R generated by the modulo operation $X \mod M$, are permutations of positive integers whose values lie in the set [0, M-1]. That is, $R = X \mod M$,so that $R \in [0, M-1], M \neq 0$.*

Theorem 5.2. *Under the symmetric model, any two radios performing SASJ achieve rendezvous in at most 4M time slots, that is $TTR = 4MT$.*

Theorem 5.3. *Under the symmetric model, ETTR of SASJ is upper bounded by*

$$ETTR = (16M - 7)/3$$

Theorem 5.4. *Under the asymmetric model, any two radios performing SASJ achieve rendezvous in at most 4M time slots with probability $Pr = G/U$, where G is the set of channels common to both radios and U the union set of channels between the two radios.*

Theorem 5.5. *Under the asymmetric model, ETTR of EJS is*

$$ETTR = \frac{G}{3U} * (25 - 16M) + \frac{16}{3} * (M - 1)$$

5.5 Theoretical Analysis

Proof of Theorem 5.1. Generally, in all computing systems or number theorems, the result of modulo operation on M is a Euclidean division whose remainder R and quotient q satisfy $q, R \in \mathbb{Z}$

$$X = M * q + R$$

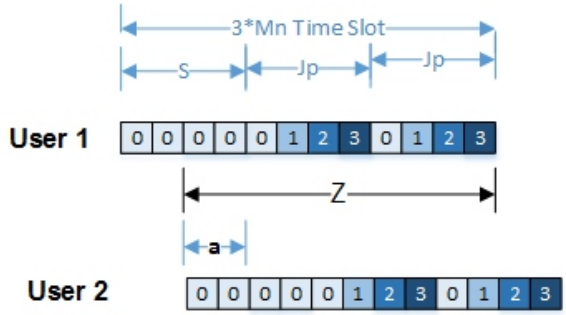

Figure 5.3: Stay-Stay Rendezvous for same channel ranking

Such that $0 \leq R < M$

Note: Based on the argument above we simply perform our SASJ CH using X mod M instead of X mod P. □

Proof of Theorem 5.2. Without loss of generality, it is assumed that SU1 begins SASJ CH sequence not later than SU2. As stated earlier that the hopping step length r is one. Recall that the channels are uniquely indexed from 0 to $(M_n - 1)$ for radio n. We consider for both symmetry and asymmetry HIA. Note that the symmetry model implies that both hopping SUs have the same channel set and asymmetry if otherwise. We look at different possible scenarios of SU2 joining the network to seek for potential rendezvous. Let Z be the length of overlap between the two radios performing SASJ algorithm. Note that TTR is considered to be the time in which all potential nodes seeking rendezvous, join the network to begin performing SASJ hopping.

Symmetric Model with same channel ranking

Here it is assumed that channels are ranked similarly for both radios such that SU1's Stay channel S, is the same as SU2's S.

Case 1 $(Z > 2M_n)$. We see in Fig. 5.3 that an overlap 'a' must exist between SU's 1 and SU's 2 stay patterns, therefore $TTR \leq M_n$ time slot.

Case 2 $(Z = 2M_n)$. The hopping sequence was generated using the modular

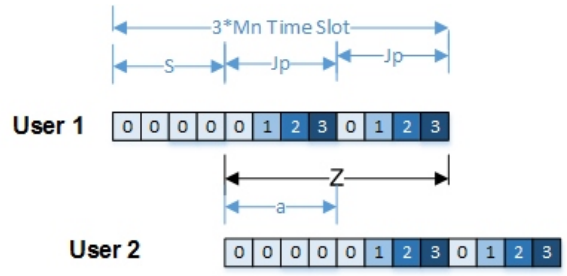

Figure 5.4: Stay-Jump Rendezvous for same channel ranking

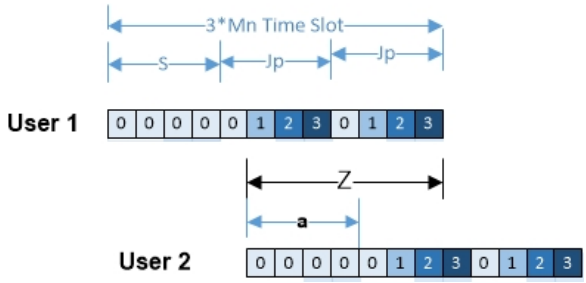

Figure 5.5: Stay-Jump Rendezvous for same channel ranking

arithmetic, as seen in section 5.3.3, as such $CH_{Jp}(n) \in M$, where M is the universal set of channels observed by SU1 and SU2, in this case of symmetry. In the interval 'a' of Fig. 5.4 rendezvous is bounded since the stay channel of SU2 ($CH_s(2)$)is a subset of the hopping sequence of SU1, $CH_{Jp}(1)$. Therefore $CH_{Jp}(1) \cap CH_s(2) \in CH_s(2)$. There is a similar analogy for case 3 ($Z < 2M_n$) and case 4 ($Z \leq M_n$) as with case 1 and 2 above. Therefore in the interval 'a' as shown in Fig.5.5 for $Z < 2M_n$, rendezvous is upper bounded within the length of the overlap. That is $TTR < 2M$ and $TTR < M$ for case 4 $Z \leq M_n$.

Symmetric Model with possibility of different channel rankings

In this case, the stay channel of SU1 and SU2 are different $S_1 \neq S_2$.

Case 5 ($Z > 2M$) This is a very interesting case as rendezvous is not always bounded in time. We introduce a modification that guarantees rendezvous in $3M + \frac{M}{2}$ time slot. Looking at Fig. 5.6 rendezvous is not guaranteed since in the interval 'a',

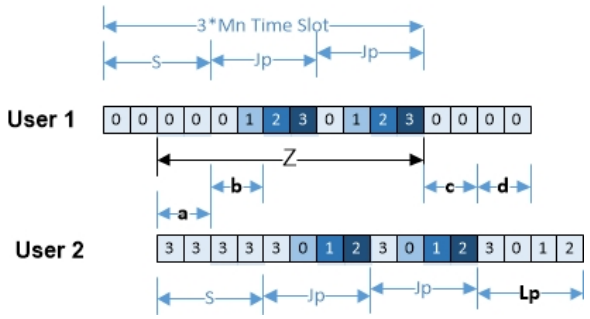

Figure 5.6: Stay-Jump Rendezvous for different channel ranking

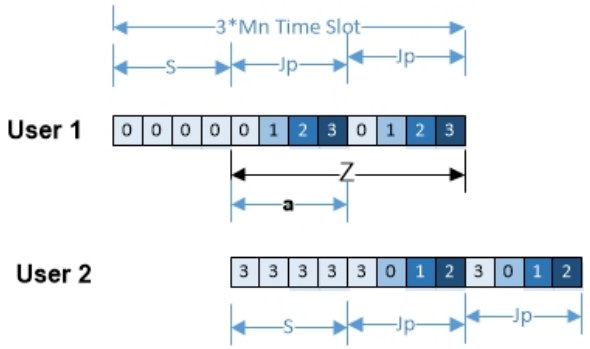

Figure 5.7: Stay-Jump Rendezvous for different channel ranking for $(Z = 2M)$

$CH_s(1) \cap CH_s(2) = \emptyset$, also for interval 'b', $CH_{Jp}(1) \cap CH_s(2) = \emptyset$ and interval 'c', $CH_{Jp}(2) \cap CH_s(1) = \emptyset$. A simple modification is to quickly run an appended hoping sequence $CH_{Lp}(2)$ in the interval d, such that $CH_{Jp}(2) \cap CH_{Lp}(2) \in M$ and $M \cap CH_s(1) \subset CH_s(1)$.

In **case 6** $(Z = 2M)$ as shown in Fig.5.7 since $CH_{Jp}(1)$ has all elements of set M and $CH_s(2) \subset M$, so rendezvous is guaranteed in $\leq M$ time slot within the interval 'a'. Therefore $TTR \leq M$ time slot. The same analogy applies for **case 7** $(M < Z < 2M)$ and **case 8** $(Z < M)$.

We see from the analysis above that, for all possible scenarios of two radios hopping across the broad spectrum TTR is upper bounded by $4M$. $TTR < 4M$

□

Proof of Theorem 5.3. We evaluate the performance of the random system using the statistical expectation estimation, described as the Expected Time to Rendezvous ETTR,

$$ETTR = \sum_{1}^{k} x_k P_k(x)$$

Since we considered eight likely scenarios, we combine the occurrence probability to determine the ETTR for the symmetric model. Since the stay channels set lies in the channel set *M*, the probability of two radios selecting same stay channel is *1/M* and the probability of selecting different stay channel is *(M-1)/M* , when user two starts hopping, the probability that user one is on its Jump or Stay pattern is 2/3, 1/3, respectively.

Therefore the ETTR for identical channel ranking is

$$ETTR(S_1 = S_2) = \frac{1}{3} * \frac{1}{M} * M + \frac{2}{3} * \frac{1}{M} * M + \frac{2}{3} * \frac{1}{M} * 2M + \frac{2}{3} * \frac{1}{M} * M \quad (5.1)$$

And for different channel ranking, it is

$$ETTR(S_1 \neq S_2) = \frac{1}{3} * \frac{M-1}{M} * 4M + \frac{2}{3} * \frac{M-1}{M} * M + \frac{2}{3} * \frac{M-1}{M} * M + \frac{2}{3} * \frac{M-1}{M} * 4M \quad (5.2)$$

The combined ETTR for our system is

$$ETTR = \frac{16M - 7}{3} \quad (5.3)$$

□

Proof of Theorem 5.4. In the asymmetric model, nodes SU1 and SU2 seeking potential channels for communication may have divergent hole information arrays, such that $M_1 \neq M_2$. G and U are defined respectively as $G = M_1 \cap M_2$ and $U = M_1 \cup M_2$. In this case, each radio constructs its hopping table and we expect rendezvous to

occur in $4U$ time slot as in symmetric model subject to the availability of common channels G. The likelihood of convergence P(C) is given as

$$P(C) = \frac{G}{U} \tag{5.4}$$

□

Proof of Theorem 5.5. Since user one and user two have M_1 and M_2 available channels with G common channels, it means they can select the same stay channel with probability $\frac{G}{U}$ and different stay channel with probability $\frac{U-G}{U}$ Therefore ETTR for an asymmetric model is given as

$$ETTR = \frac{G}{U} * ETTR(S_1 = S_2) + \frac{U-G}{U} * ETTR(S_1 \neq S_2) \tag{5.5}$$

$$ETTR = \frac{G}{3U} * (25 - 16M) + \frac{16}{3} * (M - 1) \tag{5.6}$$

□

5.6 Simulation set-up, results and discussions

The system performance evaluation was performed using MATLAB. The network parameters are in accordance with the IEEE 802.22 Standards [161]. Table 4.3 presents simulation parameters for the two-tier network. We deployed j PUs in fixed locations and n SUs randomly. The propagation environment model is that of a shadowed urban cellular radio environment with obstructed buildings. In the network the SUs use the binary geometry model described in Fig 4.2 to determine the list of available channels. The experiment was performed over 1000 iterations.

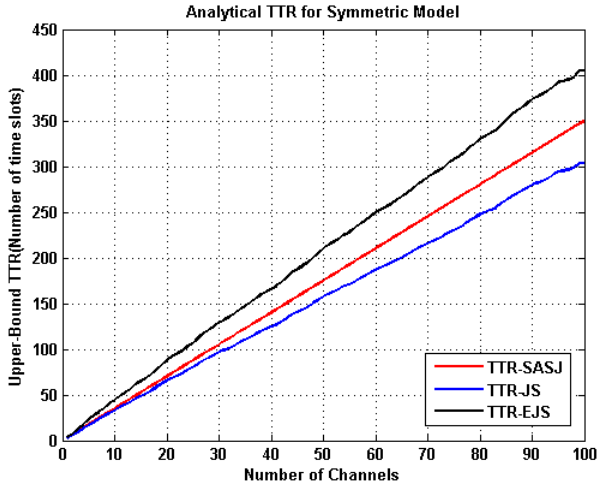

Figure 5.8: Analytical TTR for Symmetric Model

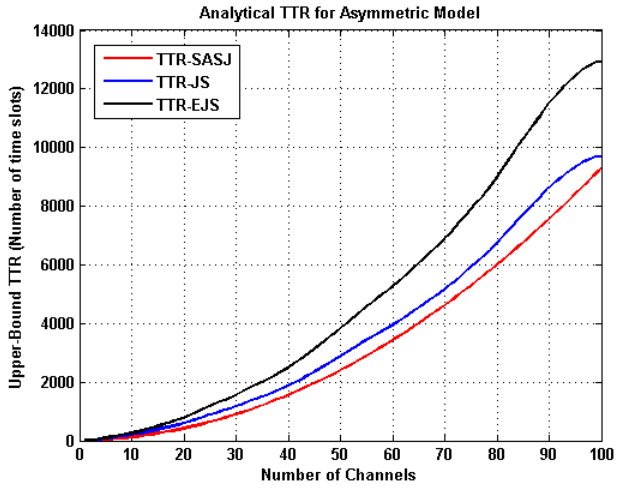

Figure 5.9: Analytical TTR for Asymmetric Model

Channels are ranked as described in subsection 4.3.3 and the SASJ algorithm was executed.

Fig 5.8 shows the analytical comparison of the SASJ TTR with that of the Enhanced Jump-Stay (EJS) and the Jump-Stay (JS) hopping Algorithm developed in [152] and [153] respectively. We see that the SASJ technique slightly outperformed the EJS regarding the reduced TTR under the symmetric model. However, it was noted that while JS did better regarding its TTR, Fig. 5.10 revealed that JS performed less

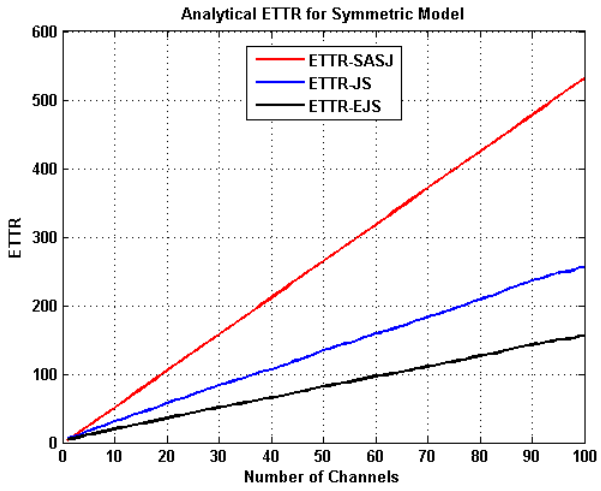

Figure 5.10: Analytical ETTR for Symmetric Model

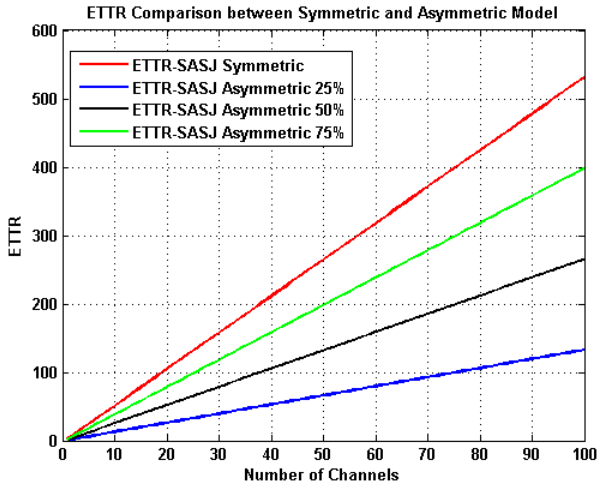

Figure 5.11: Comparison between ETTR for Symmetry and various degree of Asymmetry

when we compare its likelihood to rendezvous E(TTR) with SASJ scheme. SASJ scheme showed a higher likelihood of rendezvous under the symmetric model. Fig.5.9 shows the TTR for asymmetric model, and again the SASJ scheme showed a reduced TTR when compared with both EJ and JS. Fig.5.11 Shows a comparison of ETTR for both the symmetric model and the asymmetric model for various proportion of channel asymmetry. We see that the ETTR for the symmetric model will always

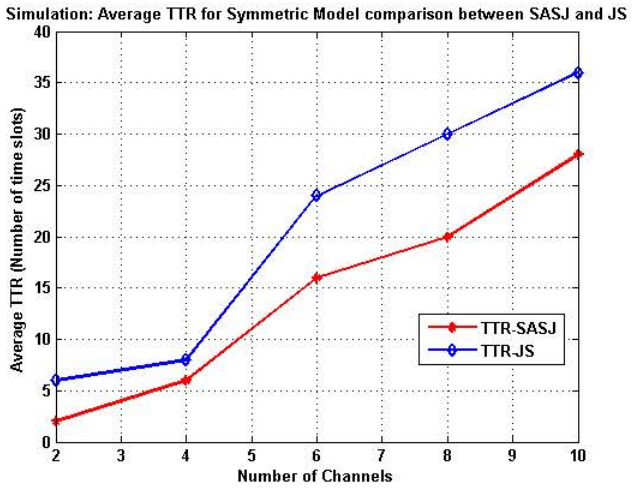

Figure 5.12: Simulation results for symmetric model: Comparing TTR for JS and SASJ

be higher than that of the asymmetric model. Fig.5.12 compared the average TTR results obtained for various runs of JS and SASJ algorithm. It was shown that overall SASJ outperforms JS.

5.7 Chapter Summary

The deployment of CR for Ad-Hoc Networks will require that nodes exchange control signals among themselves. In realising this, researchers alike agreed on the need for a dynamic control channel selection technique. This dynamic control channel selection technique offers the possibility of control channel reselection in the event of jamming or security attacks as opposed to the fixed control channel selection technique. This chapter presented a new CH scheme, the SASJ. This scheme deposits pheromone trail on its most prominent channel, updates its hole information array, rank channels and constructs CH scheme. It was shown by means of theoretical analysis and simulation that the proposed SASJ hopping scheme guarantees system rendezvous in a bounded

time. TTR and ETTR were also derived for both the asymmetric and the symmetric models. We showed an overall improvement in TTR and ETTR.

Chapter 6

Conclusion and Future Work

The concept of CR has recently gained prominence in the research communities. To this day, its realisation remains a huge challenge and has attracted series of debates which were both for and against it. CR allows for DSA and therefore remains a viable solution to the current problem of spectrum scarcity. In this thesis, we have argued in support of its realisation, exploring the promising potential of CR in an Ad-hoc network. In conclusion, this chapter has been organised as follow; Section 6.1 highlights the work achieved in this thesis and our insights on CR Ad hoc Networks. Section 6.2 elaborates on the relevant future work, and finally, the concluding remark is presented in section 6.3.

6.1 Summary

The entire thesis has focused on the development of an adaptive and autonomous MAC protocol for spectrum identification and coordination in an Ad hoc Cognitive Radio Network. In realising this, the core goal of this thesis was to develop an adaptive and an autonomous spectrum sensing technique. After that, a MAC protocol with a

flexible control channel that will guarantee efficient spectrum access and coordination for CR was developed.

Chapter 1 provided an overview of current challenges and the status quo in wireless networks. This section spanned the interest in Ad hoc networks and the CR Ad hoc networks of interest. More specifically, Chapter 1 covered the research problems targeted in this thesis and the motivations behind the investigation. In Chapter 2, background topics which are related to this thesis were reviewed.

Chapter 3 presented an Adaptive Wavelet-based Scale Space Filter (AWSSF) Algorithm for Signal detection in CR. This algorithm was based on a combination of the Wavelet-based Scale Space Filter Algorithm developed in in [132] by Xu *et al.* and the Otsu algorithm in image processing. Here Otsu's algorithm was used to introduce the adaptability for WSSF. The algorithm was tested on low SNR datasets to examine its performance. It was found that the algorithm achieved a detection rate of 90% at 10% false alarm rate, as compared to the 30% detection rate at the same false alarm rate of the ED at similar low SNR level. It was concluded that the AWSSF outperforms the ED, and can be confidently used to complement the ED in low SNR detection conditions.

Chapter 4 formulated the selection of a control channel as a path searching problem in a graph and used pheromone trail to guide the construction of an optimal solution. A step by step demonstration of the proposed control channel selection scheme using the ACS approach was described.

Chapter 5 presented the proposed CH scheme, the SASJ. This technique deposits pheromone trail on its most prominent channel updates its hole information array, rank channels and constructs CH technique. It was shown with the aid of theoretical analysis and simulation that the proposed SASJ hopping scheme guarantees system rendezvous in a bounded time. TTR and ETTR were also derived for both the

asymmetric and the symmetric models. We showed an overall improvement in TTR and ETTR.

6.2 Future Works

This thesis presented a twofold innovative approach for deploying CR technology in an Ad-hoc network. However, many open challenges and deployment issues need to be addressed to leverage potential gains of CRAHN. In the following subsections, we highlight two of these directions for future work on the critical problems discussed in this thesis.

6.2.1 Improving the edge location algorithm of AWSSF

Future works on the AWSSF may focus on improving the edge location capability of the algorithm. Besides, an extensive evaluation of the algorithm may be performed such as a complexity evaluation of the proposed AWSSF and performance comparison with more techniques in the literature.

6.2.2 Analytical evaluation of other Meta-heuristic algorithm for CC selection

In this thesis, we have explored ant colony system as an EA for channel ranking towards building a CH scheme. However, other EAs may be evaluated to analyse the convergence time, although this has not formed the focus of the study, the meta-heuristic algorithm has many drawbacks. One of the critical issues is the convergence time, which is very long compared with other analytical solution. The justification of using ant colony system may then be provided.

6.2.3 Evaluating throughput, outage probability of the CC

Extensive evaluation of the CC may be an interesting one. Other performance metrics, such as the throughput, the outage probability regarding the common control channel establishment can be evaluated.

6.3 Concluding Remarks

Different wireless communication research societies across the globe are currently involved in an intense study to develop efficient Cognitive Radio (CR) techniques. The result is to attain an effective dynamic spectrum management approach. This thesis has contributed to this very critical research area by developing an adaptive and autonomous MAC protocol for spectrum identification and coordination in Cognitive Radio. The network of interest was Ad hoc CR network. Some interesting findings were made and conclusions were drawn in this chapter.

Bibliography

Bibliography

[1] V. Cisco, "Cisco visual networking index: Global mobile data traffic forecast update, 2013-2018," *Cisco White Paper.*, 2014.

[2] T. Tjelta and R. Struzak, "Physical, technical, practical, economical and regulatory aspects of spectrum management.," *General Assembly and Scientific Symposium.*, 2011.

[3] A. J. Onumanyi, *Development of an Intelligent Hybrid Signal Detector for Enhancing Spectrum Sensing in Cognitive Radio*. PhD thesis, Federal University of Technology, Minna, 2014.

[4] M. Nekovee, "Mechanism design for cognitive radio networks," in *Complexity in Engineering, 2010. COMPENG '10.*, pp. 12–17, Feb 2010.

[5] M. T. Masonta, A. Kliks, and M. Mzyece, "Framework for tv white space spectrum access in southern african development community (sadc)," in *Personal, Indoor and Mobile Radio Communications (PIMRC Workshops), 2013 IEEE 24th International Symposium on*, pp. 133–137, Sept 2013.

[6] D. Setiawan and D. K. Hendraningrat, "Digital dividend implementation acceleration in indonesia," in *Telecommunication Systems Services and Applications (TSSA), 2014 8th International Conference on*, pp. 1–7, Oct 2014.

[7] A. Goldsmith, S. A. Jafar, I. Maric, and S. Srinivasa, "Breaking spectrum gridlock with cognitive radios: An information theoretic perspective," *Proceedings of the IEEE*, vol. 97, pp. 894–914, May 2009.

[8] B. Wang and K. J. R. Liu, "Advances in cognitive radio networks: A survey," *IEEE Journal of Selected Topics in Signal Processing*, vol. 5, pp. 5–23, Feb 2011.

[9] J. M. Peha, "Approaches to spectrum sharing," *IEEE Communications Magazine*, vol. 43, pp. 10–12, Feb 2005.

[10] Y. C. Liang, K. C. Chen, G. Y. Li, and P. Mahonen, "Cognitive radio networking and communications: an overview," *IEEE Transactions on Vehicular Technology*, vol. 60, pp. 3386–3407, Sept 2011.

[11] R. Zhou, Q. Han, R. Cooper, V. Chakravarthy, and Z. Wu, "A software defined radio based adaptive interference avoidance tdcs cognitive radio," May 2010.

[12] C. Rahman, J. Kalyanam, I. Seskar, and N. Mandayam, "Distributed spatio-temporal spectrum sensing: An experimental study," 2014.

[13] H. Y., P. J., W. W., L. J., L. K., and L. C., "A cognitive radio (cr) system employing a dual-stage spectrum sensing technique: A multi-resolution spectrum sensing MRSS and a temporal signature detection TSD technique," 2006.

[14] T. Yucek and H. Arslan, "A survey of spectrum sensing algorithms for cognitive radio applications," *Communications Surveys and Tutorials.*, vol. 11, pp. 116–130, 2009.

[15] Z. Tabakovic, S. Grgic, and M. Grgic, "Dynamic spectrum access in cognitive radio," in *ELMAR, 2009. ELMAR '09. International Symposium*, pp. 245–248, Sept 2009.

[16] S. Agarwal and S. De, "Dynamic spectrum access for energy-constrained cr: single channel versus switched multichannel," *IET Communications*, vol. 10, no. 7, pp. 761–769, 2016.

[17] B. A. F., *Cognitive Radio Technology*, vol. Vol 1. Elsevier Inc., first ed., 2006.

[18] D. Cabric, S. Mishra, and R. Brodesen, "Implementation issues in spectrum sensing for cognitive radios.," pp. 772–776, In Asilomar Conference on Signals, Systems and Computers, 2004.

[19] K. G. M. Thilina, E. Hossain, and D. I. Kim, "Dccc-mac: A dynamic common-control-channel-based mac protocol for cellular cognitive radio networks," *IEEE Transactions on Vehicular Technology*, vol. 65, pp. 3597–3613, May 2016.

[20] L. T. Tan and L. B. Le, "Multi-channel mac protocol for full-duplex cognitive radio networks with optimized access control and load balancing," in *2016 IEEE International Conference on Communications (ICC)*, pp. 1–6, May 2016.

[21] Y. Zhang, J. Zheng, and H. Chen, *Cognitive Radio Networks: Architectures, Protocols and Standards*, vol. Vol 1. CRC Press Taylor and Francis Group, first ed., 2010.

[22] C. Y. Chang, L. L. Hung, C. T. Chang, T. L. Wang, and T. C. Wang, "A cognitive radio mac protocol for exploiting bandwidth utilization in wireless networks," in *2013 9th International Wireless Communications and Mobile Computing Conference (IWCMC)*, pp. 1774–1779, July 2013.

[23] B. Dappuri, T. G. Venkatesh, and V. Thomas, "Mac protocols for cognitive radio networks with passive and active primary users," in *Wireless Communications Signal Processing (WCSP), 2013 International Conference on*, pp. 1–7, Oct 2013.

[24] B. F. Lo, "A survey of common control channel design in cognitive radio networks," *Physical Communication*, vol. 4, no. 1, pp. 26 – 39, 2011.

[25] J. Z. Yan Zhang and H.-H. Chen, *Cognitive Radio Networks: Architectures, Protocols and Standards*. CRC, 2010.

[26] J. Xiang and Y. Zhang, *Medium Access Control in Cognitive Radio Networks*, ch. Chapter 4, pp. 90–117. CRC Press Taylor and Francis Group, 2010.

[27] L. J. G. N. B. M. Ezio Biglieri, Andrea J Goldsmith, *Principles of Cognitive Radio*. Cambridge University Press, 2013.

[28] J. Lunden, V. Koivunen, and H. V. Poor, "Spectrum exploration and exploitation for cognitive radio: Recent advances," *IEEE Signal Processing Magazine*, vol. 32, pp. 123–140, May 2015.

[29] S. Haykin and P. Setoodeh, "Cognitive radio networks: The spectrum supply chain paradigm," *IEEE Transactions on Cognitive Communications and Networking*, vol. 1, pp. 3–28, March 2015.

[30] J. M. Peha, "Sharing spectrum through spectrum policy reform and cognitive radio," *Proceedings of the IEEE*, vol. 97, pp. 708–719, April 2009.

[31] Y. C. Liang, K. C. Chen, G. Y. Li, and P. Mahonen, "Cognitive radio networking and communications: an overview," *IEEE Transactions on Vehicular Technology*, vol. 60, pp. 3386–3407, Sept 2011.

[32] R. Saeed, "Cognitive radio and advanced spectrum management," in *Communications, Computers and Applications, 2008. MIC-CCA 2008. Mosharaka International Conference on*, pp. xii–xii, Aug 2008.

[33] I. F. Akyildiz, W.-Y. Lee, and K. R. Chowdhury, "Crahns: Cognitive radio ad hoc networks," *Ad Hoc Networks*, vol. 7, no. 5, pp. 810 – 836, 2009.

[34] A. V. Oppenheim and G. C. Verghese, *Signals, Systems, and Inference-Class Notes for 6.011: Introduction to Communication, Control and Signal Processing Spring 2010*. Massachusetts Institute of Technology, 2010.

[35] B. Wang and K. J. R. Liu, "Advances in cognitive radio networks: A survey," *IEEE Journal of Selected Topics in Signal Processing*, vol. 5, pp. 5–23, Feb 2011.

[36] T. Yucek and H. Arslan, "A survey of spectrum sensing algorithms for cognitive radio applications," *IEEE Communications Surveys Tutorials*, vol. 11, pp. 116–130, First 2009.

[37] Y. Xin, H. Zhang, and S. Rangarajan, "Ssct: A simple sequential spectrum sensing scheme for cognitive radio," in *Global Telecommunications Conference, 2009. GLOBECOM 2009. IEEE*, pp. 1–6, Nov 2009.

[38] A. K. Mishra, *White Space ComManagement: Advances, Developments and Engineering Challenges*. Springer, 2015.

[39] T. J.-I. P. Kimtho, "Signal detection for analog and digital tv signals for cognitive radio.," tech. rep., IEICE Technical Report (Institute of Electronics, Information and Communication Engineers)., 2006.

[40] S. Srinu, *Entropy based Reliable Cooperative Spectrum Sensing for Cognitive Radio Networks*. PhD thesis, University of Hyderabab. Central University, Hyderabah, INDIA, 2013.

[41] W. Xia, S. Wang, W. Liu, and W. Cheng, "Correlation-based spectrum sensing in cognitive radio," in *Proceedings of the 2009 ACM Workshop on Cognitive Radio Networks*, CoRoNet '09, (New York, NY, USA), pp. 67–72, ACM, 2009.

[42] S. Srinu and S. L. Saba, "FPGA implementation and performance study of spectrum sensingbased on entropy estimation using cyclic features," *Computers and Electrical Engineering Journal Elsevier*, 2010.

[43] H. Urkowitz, "Energy detection of unknown deterministic signals," *Proceedings of the IEEE*, vol. 55, pp. 523–531, April 1967.

[44] Y. C. Liang, Y. Zeng, E. C. Y. Peh, and A. T. Hoang, "Sensing-throughput tradeoff for cognitive radio networks," *IEEE Transactions on Wireless Communications*, vol. 7, pp. 1326–1337, April 2008.

[45] N. T. Ng?ethe, "An adaptive threshold energy detection technique with noise variance estimation for cognitive radio sensor networks," Master's thesis, University of Cape Town, 2015.

[46] S. K. A. P. J. R. Vesa Turunen, Marko Kosunen, "Spectrum sensor hardware implementation based on cyclostationary feature detector," *MAJLESI JOURNAL OF ELECTRICAL ENGINEERING*, 2011.

[47] S. Kandeepan, G. Baldini, and S. Dieter, "Cyclostationary feature analysis of cen-dsrc for cognitive vehicular networks," in *Intelligent Vehicles Symposium (IV), 2013 IEEE*, pp. 214–219, June 2013.

[48] O. Ugweje, "Selective noise filtration of image signals using wavelet transform," *Journal on Measurement*, 2004.

[49] S. Mallat and S. Zhong, "Characterization of signals from multiscale edge," *IEEE Transactions on Pattern Analysis and Machine Intelligence*, 1992.

[50] F. Zeng, C. Li, and Z. Tian, "Distributed compressive spectrum sensing in cooperative multihop cognitive networks," *IEEE Journal of Selected Topics in Signal Processing*, vol. 5, pp. 37–48, Feb 2011.

[51] Z. Tian and G. B. Giannakis, "Compressed sensing for wideband cognitive radios," in *2007 IEEE International Conference on Acoustics, Speech and Signal Processing - ICASSP '07*, vol. 4, pp. IV–1357–IV–1360, April 2007.

[52] D. L. Donoho, "Compressed sensing," *IEEE Transactions on Information Theory*, vol. 52, pp. 1289–1306, April 2006.

[53] J. R. Emmanuel Candes and T. Tao, "Stable signal recovery from incomplete and inaccurate measurements," *Communication Pure Applied Mathematics*, February 2005.

[54] X. Gong, *Spectrum Sensing and Interference Mitigation in Cognitive Radio Networks*. PhD thesis, Von der Fakultt fr Elektrotechnik und Informationstechnik, China, 2014.

[55] Y. Zeng and Y. C. Liang, "Eigenvalue-based spectrum sensing algorithms for cognitive radio," *IEEE Transactions on Communications*, vol. 57, pp. 1784–1793, June 2009.

[56] Y. Zeng and Y. C. Liang, "Spectrum-sensing algorithms for cognitive radio based on statistical covariances," *IEEE Transactions on Vehicular Technology*, vol. 58, pp. 1804–1815, May 2009.

[57] K. M. Thilina, K. W. Choi, N. Saquib, and E. Hossain, "Machine learning techniques for cooperative spectrum sensing in cognitive radio networks," *IEEE Journal on Selected Areas in Communications*, vol. 31, pp. 2209–2221, November 2013.

[58] C. Cortes and V. Vapnik, "Support-vector networks," *Machine Learning*, vol. 20, no. 3, pp. 273–297, 1995.

[59] A. Agostini and E. Celaya, "Reinforcement learning with a gaussian mixture model," in *The 2010 International Joint Conference on Neural Networks (IJCNN)*, pp. 1–8, July 2010.

[60] A. Kortun, T. Ratnarajah, M. Sellathurai, C. Zhong, and C. B. Papadias, "On the performance of eigenvalue-based cooperative spectrum sensing for cognitive radio," *IEEE Journal of Selected Topics in Signal Processing*, vol. 5, pp. 49–55, Feb 2011.

[61] S. Hussain and X. N. Fernando, "Performance analysis of relay-based cooperative spectrum sensing in cognitive radio networks over non-identical nakagami- m channels," *IEEE Transactions on Communications*, vol. 62, pp. 2733–2746, Aug 2014.

[62] Y. Zeng, Y.-C. Liang, A. T. Hoang, and R. Zhang, "A review on spectrum sensing for cognitive radio: Challenges and solutions," *EURASIP Journal on Advances in Signal Processing*, vol. 2010, no. 1, p. 381465, 2010.

[63] I. F. Akyildiz, B. F. Lo, and R. Balakrishnan, "Cooperative spectrum sensing in cognitive radio networks: A survey," *Phys. Commun.*, vol. 4, pp. 40–62, Mar. 2011.

[64] F. Penna, R. Garello, and M. A. Spirito, "Cooperative spectrum sensing based on the limiting eigenvalue ratio distribution in wishart matrices," *IEEE Communications Letters*, vol. 13, 2009.

[65] A. Ghasemi and E. S. Sousa, "Spectrum sensing in cognitive radio networks: requirements, challenges and design trade-offs," *IEEE Communications Magazine*, vol. 46, 2008.

[66] T. Ycek and H. Arslan, "A survey of spectrum sensing algorithms for cognitive radio applications," *IEEE Communications Surveys & Tutorials*, vol. 11, 2009.

[67] J. Unnikrishnan and V. V. Veeravalli, "Cooperative sensing for primary detection in cognitive radio," *IEEE Journal on Selected Topics in Signal Processing*, vol. 2, 2008.

[68] Y. H. Zeng and Y. . C. Liang, "Eigenvalue-based spectrum sensing algorithms for cognitive radio," *IEEE Transactions on Communications*, vol. 57, 2009.

[69] G. Ganesan and Y. Li, "Cooperative spectrum sensing in cognitive radio—part i: two user networks," *IEEE Transactions on Wireless Communications*, vol. 6, 2007.

[70] R. S.Raghave and R.Muthaiah, "Wavelet and s-transform based spectrum sensing in cognitive radio," *International Journal of Engineering and Technology*, 2003.

[71] M. Kosunen, V. Turunen, K. Kokkinen, and J. Ryynnen, "Survey and analysis of cyclostationary signal detector implementations on fpga," *IEEE Journal on Emerging and Selected Topics in Circuits and Systems*, vol. 3, pp. 541–551, Dec 2013.

[72] T. Zhang, G. Yu, and C. Sun, "Performance of cyclostationary features based spectrum sensing method in a multiple antenna cognitive radio system," in *2009 IEEE Wireless Communications and Networking Conference*, pp. 1–5, April 2009.

[73] M. H. Islam, C. L. Koh, S. W. Oh, X. Qing, Y. Y. Lai, C. Wang, Y. C. Liang, B. E. Toh, F. Chin, G. L. Tan, and W. Toh, "Spectrum survey in singapore: Occupancy measurements and analyses," in *2008 3rd International Conference on Cognitive Radio Oriented Wireless Networks and Communications (CrownCom 2008)*, pp. 1–7, May 2008.

[74] R. I. C. Chiang, G. B. Rowe, and K. W. Sowerby, "A quantitative analysis of spectral occupancy measurements for cognitive radio," in *2007 IEEE 65th Vehicular Technology Conference - VTC2007-Spring*, pp. 3016–3020, April 2007.

[75] R. Gonzalez and R. Woods, *Digital Image Processing*. Pearson Prentice Hall, 2002.

[76] W. K. Pratt, *Digital Image Processing*. john Wiley and Sons Inc., 2001.

[77] S. Barnes, P. J. van Vuuren, and B. Maharaj, "Spectrum occupancy investigation: Measurements in south africa," *Measurement*, vol. 46, no. 9, pp. 3098 – 3112, 2013.

[78] S. V. Vaseghi, *Advanced Digital Signal Processing and Noise Reduction*. John Wiley and Sons, Ltd, 2009.

[79] D. Datla, A. M. Wyglinski, and G. J. Minden, "A spectrum surveying framework for dynamic spectrum access networks," *IEEE Transactions on Vehicular Technology*, vol. 58, pp. 4158–4168, Oct 2009.

[80] F. Weidling, D. Datla, V. Petty, P. Krishnan, and G. J. Minden, "A framework for r.f. spectrum measurements and analysis," in *First IEEE International Symposium on New Frontiers in Dynamic Spectrum Access Networks, 2005. DySPAN 2005.*, pp. 573–576, Nov 2005.

[81] J. Yun, Y. Baek, J. Kim, S. Hwang, K. Cho, J. Li, K. Lee, and K. Han, "A scheduling scheme for early detection of primary user in cognitive radio networks," in *Engineering and Technology (S-CET), 2012 Spring Congress on*, pp. 1–4, May 2012.

[82] K. R. Chowdhury and I. F. Akyildiz, "Cognitive wireless mesh networks with dynamic spectrum access," *IEEE Journal on Selected Areas in Communications*, vol. 26, pp. 168–181, Jan 2008.

[83] P. Pawelczak, S. Pollin, H. S. W. So, A. Motamedi, A. Bahai, R. V. Prasad, and R. Hekmat, "State of the art in opportunistic spectrum access medium access control design," in *2008 3rd International Conference on Cognitive Radio Oriented Wireless Networks and Communications (CrownCom 2008)*, pp. 1–6, May 2008.

[84] J. Mo, H. S. W. So, and J. Walrand, "Comparison of multichannel mac protocols," *IEEE Transactions on Mobile Computing*, vol. 7, pp. 50–65, Jan 2008.

[85] P. Pawelczak, S. Pollin, H. S. W. So, A. Bahai, R. V. Prasad, and R. Hekmat, "Comparison of opportunistic spectrum multichannel medium access control protocols," in *IEEE GLOBECOM 2008 - 2008 IEEE Global Telecommunications Conference*, pp. 1–6, Nov 2008.

[86] K. R. Chowdhury and I. F. Akyldiz, "Ofdm-based common control channel design for cognitive radio ad hoc networks," *IEEE Transactions on Mobile Computing*, vol. 10, pp. 228–238, Feb 2011.

[87] B. F. Lo, I. F. Akyildiz, and A. M. Al-Dhelaan, "Efficient recovery control channel design in cognitive radio ad hoc networks," *IEEE Transactions on Vehicular Technology*, vol. 59, pp. 4513–4526, Nov 2010.

[88] M. Velempini and M. E. Dlodlo, "The analysis of multichannel mac protocols which implements a control channel," *International Journal on AdHoc Networking System*, 2014.

[89] N. Baldo, A. Asterjadhi, and M. Zorzi, "Dynamic spectrum access using a network coded cognitive control channel," *IEEE Transactions on Wireless Communications*, vol. 9, pp. 2575–2587, August 2010.

[90] L. A. DaSilva and I. Guerreiro, "Sequence-based rendezvous for dynamic spectrum access," in *New Frontiers in Dynamic Spectrum Access Networks, 2008. DySPAN 2008. 3rd IEEE Symposium on*, pp. 1–7, Oct 2008.

[91] C. Cormio and K. R. Chowdhury, "Common control channel design for cognitive radio wireless ad hoc networks using adaptive frequency hopping," *Ad Hoc Networks*, vol. 8, no. 4, pp. 430 – 438, 2010.

[92] N. C. Theis, R. W. Thomas, and L. A. DaSilva, "Rendezvous for cognitive radios," *IEEE Transactions on Mobile COmputing*, 2011.

[93] K. Bian, J.-M. Park, and R. Chen, "A quorum-based framework for establishing control channels in dynamic spectrum access networks," in *Proceedings of the 15th Annual International Conference on Mobile Computing and Networking*, MobiCom '09, (New York, NY, USA), pp. 25–36, ACM, 2009.

[94] T. Chen, H. Zhang, G. M. Maggio, and I. Chlamtac, "Topology management in cogmesh: A cluster-based cognitive radio mesh network," in *2007 IEEE International Conference on Communications*, pp. 6516–6521, June 2007.

[95] L. Le and E. Hossain, "A mac protocol for opportunistic spectrum access in cognitive radio networks," in *2008 IEEE Wireless Communications and Networking Conference*, pp. 1426–1430, March 2008.

[96] B. Hamdaoui and K. G. Shin, "Os-mac: An efficient mac protocol for spectrum-agile wireless networks," *IEEE Transactions on Mobile Computing*, vol. 7, pp. 915–930, Aug 2008.

[97] H. Su and X. Zhang, "Cross-layer based opportunistic mac protocols for qos provisionings over cognitive radio wireless networks," *IEEE Journal on Selected Areas in Communications*, vol. 26, pp. 118–129, Jan 2008.

[98] H. Su and X. Zhang, "Opportunistic mac protocols for cognitive radio based wireless networks," in *2007 41st Annual Conference on Information Sciences and Systems*, pp. 363–368, March 2007.

[99] L. Ma, X. Han, and C.-C. Shen, "Dynamic open spectrum sharing mac protocol for wireless ad hoc networks," in *First IEEE International Symposium on New Frontiers in Dynamic Spectrum Access Networks, 2005. DySPAN 2005.*, pp. 203–213, Nov 2005.

[100] H. Su and X. Zhang, "Cream-mac: An efficient cognitive radio-enabled multi-channel mac protocol for wireless networks," in *World of Wireless, Mobile and Multimedia Networks, 2008. WoWMoM 2008. 2008 International Symposium on a*, pp. 1–8, June 2008.

[101] A. Rahimi-Vahed and A. H. Mirzaei, "A hybrid multi-objective shuffled frog-leaping algorithm for a mixed-model assembly line sequencing problem," *Computers & Industrial Engineering*, vol. 53, no. 4, pp. 642 – 666, 2007.

[102] A. Kaveh and S. Talatahari, "Particle swarm optimizer, ant colony strategy and harmony search scheme hybridized for optimization of truss structures," *Computers & Structures*, vol. 87, no. 56, pp. 267 – 283, 2009.

[103] P. Shelokar, P. Siarry, V. Jayaraman, and B. Kulkarni, "Particle swarm and ant colony algorithms hybridized for improved continuous optimization," *Applied Mathematics and Computation*, vol. 188, no. 1, pp. 129 – 142, 2007.

[104] E. Elbeltagi, T. Hegazy, and D. Grierson, "Comparison among five evolutionary-based optimization algorithms," *Advanced Engineering Informatics*, vol. 19, no. 1, pp. 43 – 53, 2005.

[105] H. Ahmed and J. Glasgow, "Swarm intelligence: Concepts, models and applications," tech. rep., School of Computing Queen's University Kingston, Ontario, Canada, 2012.

[106] A. Shmygelska and H. H. Hoos, "An ant colony optimisation algorithm for the 2d and 3d hydrophobic polar protein folding problem," *BMC Bioinformatics*, vol. 6, no. 1, pp. 1–22, 2005.

[107] C. Blum, "Beam-aco?hybridizing ant colony optimization with beam search: an application to open shop scheduling," *Computers & Operations Research*, vol. 32, no. 6, pp. 1565 – 1591, 2005.

[108] C. Blum, J. Bautista, and J. Pereira, *Ant Colony Optimization and Swarm Intelligence: 5th International Workshop, ANTS 2006, Brussels, Belgium,*

September 4-7, 2006. Proceedings, ch. Beam-ACO Applied to Assembly Line Balancing, pp. 96–107. Berlin, Heidelberg: Springer Berlin Heidelberg, 2006.

[109] L. M. Gambardella and M. Dorigo, "An ant colony system hybridized with a new local search for the sequential ordering problem," *INFORMS J. on Computing*, vol. 12, pp. 237–255, July 2000.

[110] T. S. Z. Y. Prasanna Balaprakash, Mauro Birattari and M. Dorigo, "Estimation-based ant colony optimization and local search for the probabilistic traveling salesman problem," *Springer Science Swarm Intell*, 2009.

[111] C. Blum, M. Y. Vall?s, and M. J. Blesa, "An ant colony optimization algorithm for {DNA} sequencing by hybridization," *Computers & Operations Research*, vol. 35, no. 11, pp. 3620 – 3635, 2008. Part Special Issue: Topics in Real-time Supply Chain Management.

[112] O. Korb, T. Stützle, and T. E. Exner, "An ant colony optimization approach to flexible protein–ligand docking," *Swarm Intelligence*, vol. 1, no. 2, pp. 115–134, 2007.

[113] V. Roberge, M. Tarbouchi, and G. Labonte, "Comparison of parallel genetic algorithm and particle swarm optimization for real-time uav path planning," *IEEE Transactions on Industrial Informatics*, vol. 9, pp. 132–141, Feb 2013.

[114] R. Dawkins, *The selfish gene.* Oxford., 1976.

[115] H. F., "Selfish memes and the evolution of cooperation," *J. Ideas*, vol. 2, p. 77, 1992.

[116] M. P and F. B., "A genetic local search approach to the quadratic assignment problem.," in *Proceedings of the 7th international conference on genetic algorithms. San Diego, CA: Morgan Kaufmann.*, 1997. p. 46572.

[117] P. Moscato and M. G. Norman, "A memetic approach for the traveling salesman problem implementation of a computational ecology for combinatorial optimization on message-passing systems," *International conference on parallel computing and transputer application. Amsterdam, Holland:*, 1992.

[118] J. Kennedy and R. Eberhart, "Particle swarm optimization," in *Neural Networks, 1995. Proceedings., IEEE International Conference on*, vol. 4, pp. 1942–1948 vol.4, Nov 1995.

[119] Y. Shi and R. Eberhart, "A modified particle swarm optimizer," in *1998 IEEE International Conference on Evolutionary Computation Proceedings. IEEE World Congress on Computational Intelligence (Cat. No.98TH8360)*, pp. 69–73, May 1998.

[120] Eberhart and Y. Shi, "Particle swarm optimization: developments, applications and resources," in *Proceedings of the 2001 Congress on Evolutionary Computation (IEEE Cat. No.01TH8546)*, vol. 1, pp. 81–86 vol. 1, 2001.

[121] M. Eusuff, K. Lansey, and F. Pasha, "Shuffled frog-leaping algorithm: a memetic meta-heuristic for discrete optimization," *Engineering Optimization*, vol. 38, no. 2, pp. 129–154, 2006.

[122] R. C. W., "Flocks, herds and schools: a distributed behavioral model," *Comput. Graphics*, vol. 21, p. 25, 1987.

[123] S.-Y. Liong and M. Atiquzzaman, "Optimal design of water distribution network using shuffled complex evolution.," *Journal of The Institution of Engineers, Singapore*, 2004.

[124] H. Ohize, M. Dlodlo, A. J. Onumanyi, and H. Bello-Salau, "An adaptive wavelet-based scale space filtering algorithm for spectrum sensing in cognitive

radio," in *Wireless Communications and Networking Conference (WCNC), San Francisco, USA*, 2017.

[125] C. VSN, "Cisco visual networking index: Global mobile data traffic forecast update, 2015?2020 white paper," *Cisco*, 2016.

[126] H. Ohize and M. Dlodlo, "Ant colony system based control channel selection scheme for guaranteed rendezvous in cognitive radio ad-hoc network," in *27th Annual IEEE International Symposium on Personal, Indoor and Mobile Radio Communications - (PIMRC)*, 2016.

[127] N. Wang, Y. Gao, and L. Cuthbert, "Spectrum sensing using adaptive threshold based energy detection for ofdm signal," in *IEEE International Conference on Communication Systems*, 2014.

[128] Z. Tian and G. Giannakis, "A wavelet approach to wideband spectrum sensing for cognitive radio," in *Cognitive Radio Oriented Wireless Networks and Communications*, 2006.

[129] K. Divakaran, N. Manikandan, and H. Shri, "Wavelet based spectrum sensing techniques for cognitive radio-a survey," *International Journal of Computer Science & Information Technology*, vol. 3, pp. 123–137, April 2011.

[130] Y.-L. Xu, H.-S. Zhang, and Z.-H. Han, "The performance analysis of spectrum sensing algorithms based on wavelet edge detection," in *International Conference on Wireless Communications, Networking and Mobil Computing*, 2009.

[131] Y. Zhao, Y. Wu, J. Wang, X. Zhong, and L. Mei, "Wavelet transform for spectrum sensing in cognitive radio networks," in *International Conference*

on Audio, Language and Image Processing., (Shanghai), pp. 565–569, IEEE, International Conference, July 2014.

[132] Y. Xu, J. B. Weaver, D. M. Healy, and J. Lu, "Wavelet transform domain filters: a spatially selective noise filtration technique," *IEEE Transactions on Image Processing*, vol. 3, pp. 747–758, Nov 1994.

[133] Y. Zheng, D. B. Tay, and L. Li, "Signal extraction and power spectrum estimation using wavelet transform scale space filtering and bayes shrinkage," *Signal Processing*, vol. 80, no. 8, pp. 1535 – 1549, 2000.

[134] O. Nobuyuki, "A threshold selection method from gray-level histograms," *IEEE Transactions on Systems, Man and Cybernetics*, 1979.

[135] T. Fawcett, "An introduction to roc analysis," *Pattern Recogn. Lett.*, vol. 27, pp. 861–874, June 2006.

[136] R. Rao, Q. Cheng, and P. Ray, "Subspace-based cooperative spectrum sensing for cognitive radio," in *2008 42nd Asilomar Conference on Signals, Systems and Computers*, pp. 1662–1666, Oct 2008.

[137] D. Sundararajan, "Fundamentals of the discrete haar wavelet transform," 2011.

[138] M. U. Micheal Vrhel, Chulhee Lee, "Fast continuous wavelet transform," *Biomedical Engineering and Instrumentational Program, National Institute of Health, Belthesda*, 1995.

[139] H. Ohize and M. Dlodlo, "Dynamic control channel mac for cognitive radio ad-hoc network: Ant colony system implementation." submited to SATNAC 2016.

[140] C. Cormio and K. R. Chowdhury, "An adaptive multiple rendezvous control channel for cognitive radio wireless ad hoc networks," in *Pervasive Computing*

and Communications Workshops (PERCOM Workshops), 2010 8th IEEE International Conference on, pp. 346–351, March 2010.

[141] M. Dorigo and L. M. Gambardella, "Ant colony system: A cooperative learning approach to the traveling salesman problem," *IEEE Transaction on Evolutionary Commputation*, 1997.

[142] Q. He and P. Zhang, "Dynamic channel assignment using ant colony optimization for cognitive radio networks," in *Vehicular Technology Conference (VTC Fall), 2012 IEEE*, pp. 1–5, Sept 2012.

[143] F. Koroupi, S. Talebi, and H. Salehinejad, "Cognitive radio networks spectrum allocation: An {ACS} perspective," *Scientia Iranica*, vol. 19, pp. 767 – 773, jun 2012.

[144] D. S. Weile and E. Michielssen, "Genetic algorithm optimization applied to electromagnetics: a review," *IEEE Transactions on Antennas and Propagation*, vol. 45, pp. 343–353, Mar 1997.

[145] L. L. Chung-Wei Feng and S. A. Burns, "Stochastic construction time-cost trade-off analysis," *Stochastic Construction Time-Cost Trade-Off Analysis*, 2004.

[146] T. Hegazy, "Optimization of construction time-cost trade-off analysis using genetic algorithms," *Canadian Journal of Civil Engineering*, vol. 26, no. 6, pp. 685–697, 1999.

[147] M. M. Eusuff and K. E. Lansey, "Optimization of water distribution network design using the shuffled frog leaping algorithm.," *Journal of Water Resources Planning and Management*, 2003.

[148] H. R. Maier, A. R. Simpson, A. C. Zecchin, W. K. Foong, K. Y. Phang, H. Y. Seah, and C. L. Tan, "Ant colony optimization for design of water distribution systems," *Journal of Water Resources Planning and Management*, 2003.

[149] T. Rappaport, *Wireless Communications Principles and Practice*. The Prentice Hall, 2010.

[150] M. Okwori, M. Bima, O. Inalegwu, M. Saidu, W. Audu, and U. Abdullahi, "Energy efficient routing in wireless sensor network using ant colony optimization and firefly algorithm.," in *International Conference on Information and Communication Technology and Its Applications (ICTA 2016)*, 2016.

[151] B. Horine and D. Turgut, "Link rendezvous protocol for cognitive radio networks," in *2007 2nd IEEE International Symposium on New Frontiers in Dynamic Spectrum Access Networks*, pp. 444–447, April 2007.

[152] H. Liu, Z. Lin, X. Chu, and Y.-W. Lueng, "Jump-stay rendezvous algorithm for cognitive radio networks," *IEEE Transactions on Parallel and Distributed Systems*, 2012.

[153] Z. Lin, H. Liu, X. Chu, and Y.-W. Lueng, "Enhanced jump-stay rendezvous algorithm for cognitive radio networks," *IEEE Communications Letters*, 2013.

[154] I. Chuang, H. Y. Wu, K. R. Lee, and Y. H. Kuo, "Alternate hop-and-wait channel rendezvous method for cognitive radio networks," in *INFOCOM, 2013 Proceedings IEEE*, pp. 746–754, April 2013.

[155] I.-H. Chuang and H.-Y. a. Y.-H. Wu, "A fast blind rendezvous method by alternate hop-and-wait channel hopping in cognitive radio networks," *IEEE Transactions on Mobile Computing*, 2014.

[156] H. Liu, Z. Lin, X. Chu, and Y. W. Leung, "Ring-walk based channel-hopping algorithms with guaranteed rendezvous for cognitive radio networks," in *Green Computing and Communications (GreenCom), 2010 IEEE/ACM Int'l Conference on Int'l Conference on Cyber, Physical and Social Computing (CPSCom)*, pp. 755–760, Dec 2010.

[157] G.-Y. Chang, W.-H. Teng, H.-Y. Chen, and J.-P. Sheu, "Novel channel-hopping schemes for cognitive radio networks," *IEEE Transactions on Mobile Computing*, 2014.

[158] F. Hou, L. X. Cai, X. Shen, and H. Jianwei, "Asynchronus multichannel MAC design with difference-set-based hopping sequence," *IEEE Transactions on Vehicular Technology*, 2011.

[159] Z. Gu, Q.-S. Hua, Y. Wang, and F. C. M. Lau, "Nearly optimal asynchronous blind rendezvous algorithm for cognitive radio networks," in *2013 IEEE International Conference on Sensing, Communications and Networking (SECON)*, pp. 371–379, June 2013.

[160] C. M. Chao and H.-Y. Fu, "Providing complete rendezvous guarantee for cognitive radio networks by quorum systems and latin squares," in *2013 IEEE Wireless Communications and Networking Conference (WCNC)*, pp. 95–100, April 2013.

[161] C. R. Stevenson, G. Chouinard, Z. Lei, W. Hu, S. Shellhammer, and W. Caldwell, "Ieee 802.22: The first cognitive radio wireless regional area network standard," *IEEE COmmunications Magazine*, 2009.

Appendices

Appendix A

Codes for the AWSSF

Table of Contents


```
close all; clc; clear;
global wname level upthresh winsig sorh numofdata ds
```

Real Data

dataset = ((xlsread('FM_1000_90_94')'); min_data = -1*(min(dataset(2,:))); Pav = min_data + (dataset(2,:)); figure plot(Pav) % dataset(1,:), xlabel('Frequency (Hz)'); ylabel('Power (dBm)'); ad_data = Pav;

Simulated Data

```
load('SNR_band_one_dB')
Pav = PSD(5:end);
% tt = multithresh(Pav,2)
% [threshold,thres_data,bins] = mod_otsu_main(Pav);
figure
plot(Pav)
% hold on
% plot(1:length(Pav),tt(2),'r')
% hold on
% plot(1:length(Pav),threshold,'g')
ad_data = Pav;
```

Generate Ground Truth Data here

```
g = length(Pav);
ground_truth = Pav(1:g);
% ================================
GT = zeros(1,length(ground_truth));
% GT(270:288) = 1; GT(512:548) = 1; % For the Real Data
% GT(95:199) = 1;
GT(240:313) = 1;
```

Processing Section

```
wname = 'haar';
level = 6;
ad = mod(length(Pav),2^level);
```

```
if ad > 0
    Pav = [Pav,zeros(1,(2^level - ad))];
end
% actualsig = dataset';
save('spectrum_data','Pav')
% for th = 0.01
    [~,wDECd] = swt(Pav',level,wname);
    for bb = 1:level
        wDECd(bb,g-20:g) = 0;
    end
    wDECSHORT = wDECd(1:level,1:g);
    for vv = 1:level
        figure
        plot(wDECSHORT(vv,:))
        xlabel('Signal Index'); ylabel('Wavelet Coefficient')
        title(['The Wavelet Coefficients for',' ','Level',' ','=',' ',num2str(vv)]
    end
    [sf,th] = spacescaletest(Pav(1:g),wname,level,wDECSHORT,sorh,GT);
% end
noise_floor = min(ground_truth);
for ss = 1:g
    if sf(ss) == 0
        Pav(ss) = noise_floor;
    else
        Pav(ss) = Pav(ss);
    end
end
filtered_sig = Pav(1:g);
```

Analysis Stage:

```
for ss = 1:g
    if GT(ss) == 0
        ground_truth(ss) = noise_floor;
    else
        ground_truth(ss) = ground_truth(ss);
    end
end
figure
plot(ground_truth)
title('Groundtruth Signal')
figure
plot(filtered_sig)
title('Filtered Signal')
NN = length(find(ground_truth == noise_floor))
SS = g - NN;
```

Perform ROC analysis here

```
figure
plot(GT)
roc_plot_final(GT,ad_data)
roc_plot_final(GT,filtered_sig)
```

Published with MATLAB® R2013a

Appendix B

Codes for the ACO Algorithm

```
%This will applies ACO to select the optimal common channel between
 two nodes
clear;
clc;
```

initialization

```
%declaring model for the nest
model=CreateModel();

CostFunction = @(ant) CostFxn(ant,model);

%Creating the ants
ant.choice=[];
ant.ld=[];
ant.cost=0;
ant.s=[];
ant.d=[];

no_of_ant=50;
ant=repmat(ant,1,no_of_ant);

%pheromone_trail initialization, Column 1 = decision point i and
 column 2=
%decision point j
i = length(model.i);
j = length(model.j);
cha = length(model.ch);
tau=ones(i,j,cha);

alpha=0.3;      % Phromone Exponential Weight

rho=0.1;        % Evaporation Rate

%1000 iterations
maxit=1000;
BestCost=zeros(maxit,1);

BestSol.cost=0;
Bestcount=0;

no_of_nodes=length(model.i);
node1 = abs(round((0.5+(0.5*rand(1,no_of_nodes)))*no_of_nodes));
node2 = abs(round((0.5+(0.5*rand(1,no_of_nodes)))*no_of_nodes));

%get distance betweeen nodes and set the linking distance ld
D=model.D;
ld=200;

%Time to move the ants
for i=1:maxit
    for j=1:no_of_ant
```

```
        %Creating the ants
         ant(j).choice=[];
         ant(j).ld=[];
         ant(j).cost=0;
         ant(j).s=[];
         ant(j).d=[];

         for k=1:no_of_nodes
         %select channel between nodes n and m
            m=node1(k);
            n=node2(k);
            %check if nodes are within range
            if D(n,m)<=ld
            %extract the pheromone trail for all channels between nodes
n
            %and m
                P=getPheromone(m,n,tau).^alpha;
                %check for common channels
                C=getChannels(n,m,model);
                P=P.*C';
                P=P/sum(P);
                sel=0;
                if n~=m
                sel=RouletteWheelSelection(P);
                end
                ant(j).choice(k)=sel;
                ant(j).ld(k)=1;
                ant(j).s(end+1)=m;
                ant(j).d(end+1)=n;

            end
         end
            CF=CostFunction(ant(j));
            ant(j).cost=CF;


            %determine the best route
            if ant(j).cost>=BestSol.cost
            BestSol=ant(j);
            end
   end
    %Update Phromone

    for k=1:no_of_ant

         choice=ant(k).choice;

         for l=1:no_of_nodes
             s=node1(l);
             d=node2(l);
             if choice(l)~=0
             tau(s,d,choice(l))=tau(s,d,choice(l))+ant(k).cost;
             end
```

```
        end

    end


    %Evaporation
    tau=(1-rho)*tau;
    %tau(tau<0.1)=0.1;

    BestCost(i)=BestSol.cost;

    % Show Iteration Information
    disp(['Iteration ' num2str(i) ': Best Cost = '
 num2str(BestCost(i))]);
end
```

Published with MATLAB® R2015a

```
% This computes the cost/reward/objective function
function R=CostFxn(ant,model)
        %a is the range factor
        %c specifies whether nodes n,k have a common channel
        %b specifies channel capacity
        %note, a,c and b must be same dimension
        %format for the tour is [i,j]
        a=ant.ld;
        c=ant.choice;
        s=ant.s;
        d=ant.d;
        %incase a zero is chosen between two nodes, use a 1 to avoid
        %subscript indices error
        c1=c==0;
        c2=c+c1;
        b=zeros(length(c),1);
        for j=1:length(c)
            b(j)=model.cap(s(j),d(j),c2(j));
        end
        b1=zeros(length(c),1);
        for j=1:length(c)
            b1(j)=b(j,1);
        end
        c1=c>0;
        b1=b1.*c1';
        R=0;
        R1=a'.*(c'.*b1);
        R=sum(sum(R1,1));
end
```

Published with MATLAB® R2015a

```
% This creats the network model
function model=CreateModel()
%Simply return the channel matrix
%The placement of nodes has been done randomly and so is the channel
%creation
ch=round(rand(1,10)*7000);
i=round(rand(1,10)*100);
j=round(rand(1,10)*100);
D=zeros(length(i));
for k=1:length(i)
    for l=k+1:length(j)
        D(k,l)= sqrt((i(k)-i(l))^2 + (j(k)-j(l))^2);
        D(l,k)=D(k,l);
    end
end
model.D=D;
model.i=i;
model.j=j;
%Allocate availability between nodes randomly
c= rand(length(i),length(j),length(ch))>0.5;

model.c=c;
%Channel capacity between nodes
%need to calculate the channnel capacity between nodes
%using random and normalized values for now.
%Mr Henry will need to provide the details for this calculation
sigma=8;
A=6;
d_ij=repmat(D, [1 1 length(ch)]);
g=3.76;
B_0=6;

sh_dB_km=sigma*randn(length(i),length(j),length(ch));
y_ij=A-10*g*log10(d_ij)+sh_dB_km;
alpha=-1.5/log(5);
b_ij=B_0*log2(1+alpha*y_ij);

cap=real(b_ij);
cap(isinf(cap))=0;

model.cap=cap;
model.ch=ch;
end
```

Published with MATLAB® R2015a

```
% This computes the cost/reward/objective function
function R=CostFxn(ant,model)
        %a is the range factor
        %c specifies whether nodes n,k have a common channel
        %b specifies channel capacity
        %note, a,c and b must be same dimension
        %format for the tour is [i,j]
        a=ant.ld;
        c=ant.choice;
        s=ant.s;
        d=ant.d;
        %incase a zero is chosen between two nodes, use a 1 to avoid
        %subscript indices error
        c1=c==0;
        c2=c+c1;
        b=zeros(length(c),1);
        for j=1:length(c)
            b(j)=model.cap(s(j),d(j),c2(j));
        end
        b1=zeros(length(c),1);
        for j=1:length(c)
            b1(j)=b(j,1);
        end
        c1=c>0;
        b1=b1.*c1';
        R=0;
        R1=a'.*(c'.*b1);
        R=sum(sum(R1,1));
end
```

Published with MATLAB® R2015a

```
% Pheromone update
function coll = getPheromone(n,k, tau)
col=zeros(size(tau,3),1);
for l=1:length(col)
    col(l)= tau(n,k,l);
end
coll=col;
end
```

Published with MATLAB® R2015a

```
function j=RouletteWheelSelection(P)
    r=rand;
    C=cumsum(P);
    j=find(r<=C,1,'first');
end
```

Published with MATLAB® R2015a